KTH Industrial Engineering and Management

Designing battery thermal management systems(BTMS) for cylindrical Lithium-ion battery modules using CFD

Seyed Mazyar Hosseini Moghaddam

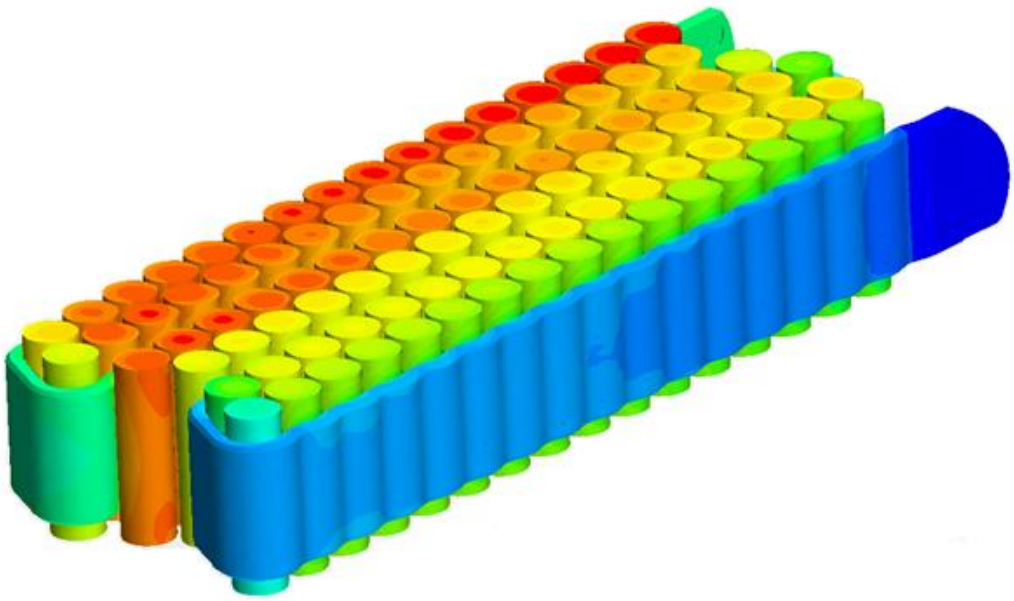

Master of Science Thesis
KTH School of Industrial Engineering and Management
Energy Technology: TRITA-ITM-EX 2018:636
SE-100 44 STOCKHOLM

Master of Science Thesis: TRITA-ITM-EX 2018:636

KTH Industrial Engineering and Management

Designing thermal management systems for Lithium-ion battery modules using CFD

Seyed Mazyar Hosseini Moghaddam

Approved	Examiner	Supervisor
2019-02-04	Reza Fakhrai	Ehsan Haghighi Bitaraf
	Commissioner	Contact person

Abstract

Renewable Energies have the capability to cut down the severe impacts of energy and environmental crisis. Integrating renewable energy generation into the global energy system calls for state of the art energy storage technologies. The lithium-ion battery is introduced in this paper as a solution with a promising role in the storage sector on the grounds of high mass and volumetric energy density. Afterward, the advantages of proper thermal management, including thermal runaway prevention, optimum performance, durability, and temperature uniformity are described. In particular, this review detailedly compares the most frequently adopted battery thermal management solutions (BTMS) in the storage industry including direct and indirect liquid, air, phase-change material, and heating.

In this work, four battery thermal management solutions are selected and analyzed using Computational Fluid Dynamic (CFD) simulations for accurate thermal modeling. The outcome of the simulations is compared using parameters e.g. temperature distribution in battery cells, battery module, and power consumption. Liquid cooling utilizing the direct contact higher cooling performance to the conventional air cooling methods. However, there exist some

challenges being adopted in the market. Each of the methods proves to be favorable for a particular application and can be further optimized.

Sammanfattning

Integrering av förnybara energier i globala energisystem kräver enorma energilagrings teknologier. Litium jon batterier spelar en viktig roll inom denna sektor på grund av både hög vikt- och volymmässig energidensitet. Korrekt värmestyrning (Thermal management) är nödvändigt för litium jon batteriernas livslängd och operation. Dessa batterier fungerar bäst när de ligger inom intervallet 15–35 grader. dessutom har olika värmestyrsystem utvecklats för att säkerställa att batterierna arbetar optimalt i olika applikationer.

I den här studien fem värmestyrningslösningar för batterier har väljas och analyseras med hjälp av beräkningsvätskedynamik (CFD) simulering. Resultaten av simuleringarna jämförs med olika parametrar som temperaturfördelning i battericeller, batterimoduler och strömförbrukning. Alla metoder visar sig vara användbara lämplig för viss tillämpning och kan vidare optimeras för detta ändamål.

Contents

1. Introduction

The rise of renewable power generation in the current energy market has created an immense potential for different forms of energy storage. At the forefront of these storage technologies are the lithium batteries as they are lightweight with high energy density. The characteristics of Lithium batteries have made them attractive both for stationary and automotive applications. However, despite their promising future, there are major hindrances with regards to a battery system e.g. safety concerns, cost, limited calendar life, and temperature related issues. Temperature has a large effect on the safety, lifetime and performance of Li-ion batteries. The optimum operating range for these batteries is 15-35^{o}C [1] otherwise the performance and lifespan will be reduced and furthermore hazardous incidents such as thermal runaway might occur. In addition, temperature difference among cells and modules in a battery pack must be controlled, else it will impact the operation and aging of the battery. Thus, an effective battery thermal management system is necessary to dissipate the heat generated inside the batteries. Moreover, in low-temperature scenarios, heating is required to ensure the best performance.

This project aims to analyze and compare the performance of different cooling methods used for thermal management of lithium battery modules consisting of 21700 cylindrical cells. The comparison is done by simulating the performance of a 96 cell module using computational fluid dynamic software Star-CCM+. The software replicates the flow distribution and various properties of the cells and the media around them. To analyze the results certain criteria such as maximum temperature in a module, coolants temperature rise, the temperature distribution within each cell and modules are compared to each other.

2. Background

2.1. Li-ion batteries

Li-ion batteries consist of lithium in the positive electrode and electrolyte where lithium ions move from positive to negative electrode during charging and vice versa during discharge. What gives leverage to lithium-ion batteries compared to other battery technologies is their volumetric and mass energy density. This feature makes lithium-ion batteries very attractive for different applications, especially the automotive industry where the energy density is critical.

Lithium Batteries are manufactured in three different form factors namely cylindrical, prismatic and pouch. In cylindrical cells, the layers are rolled and put into a cylindrical can Figure 1. The advantage of this cell format is mechanical stability and ease of manufacturing. Prismatic cell Figure 12 is wrapped in packages for thinner design demands. They are mainly found in electronic devices such as mobile phones. Pouch cells have the most efficient packaging by eliminating the metal enclosure and allow stacking.

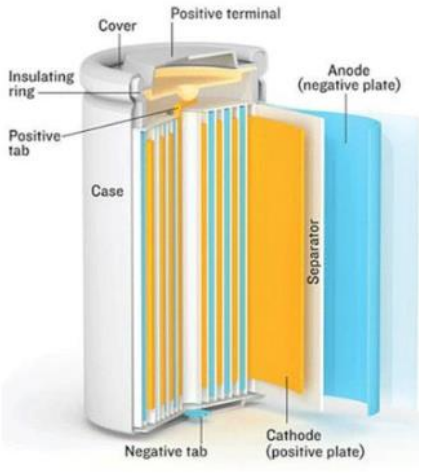

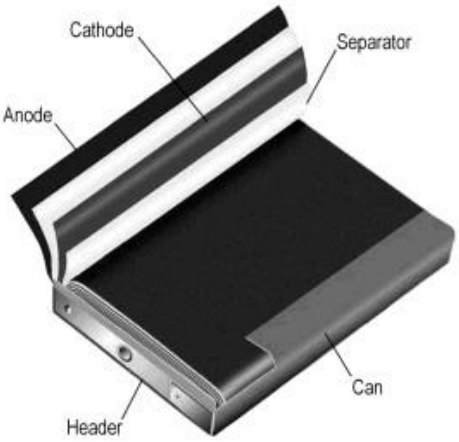

Figure 1. Lithium-ion cylindrical cell composition [2] *Figure 2. Lithium-ion prismatic cell composition [3]*

Figure 3. Lithium-ion pouch cell composition [3]

The focus of this report has been on cylindrical cells. To explore the issues regarding the thermal management of lithium batteries, most effectively, a subset of literature has been selected based on the following question.

1. How is heat generated in a battery?
2. How does a battery thermal management (BTM) improve the performance of the Li-ion battery cells?
3. What are the different methods used for BTM for Li-ion cells?
4. How can the thermal properties of a battery be measured?

There are several scientific papers published with the aim of answering each of the issues presented in details. This review focuses on the more recent pieces of literature hoping to provide a sounder understanding of the Li-ion thermal management.

2.2. Heat generated inside the batteries

Battery cooling is directly proportional to the heat generated inside them, thus it is important to know where the heat comes from. Bernardi et al. Used a thermodynamic energy balance to drive a formula for the heat generated inside a battery. He considers four processes that affect this balance. First is the electrical power that is produced inside the battery and the second is reversible reactions and entropic heating from them. Below is a reaction in a typical Lithium-ion battery. The square represents the empty site for the lithium-ion [4].

$$LiCoO_2 + \blacksquare C_6 \leftrightarrows \blacksquare CoO_2 + LiC_6$$

The third process is the heat produced from the mixing due to the variation of the concentration of the battery as the reaction develops. The last process in the energy balance is the heat dissipated from the phase changes of the materials.

In most literature, the Bernali equation is simplified and presented as:

$$q = I(U - V) - I(T\frac{\partial U}{\partial T}) \quad \textit{Eq. 1}$$

In this phrase, the heat of mixing and phase change are neglected. The first term represents the overpotentials during charge transfer at the interface and ohmic losses. The second term is the reversible entropic heat from the reaction [5].

2.3. Thermal management impact on battery performance

Performance of lithium-ion cell is very dependent on the temperature of the cell. Lithium batteries have an optimum working temperature at 15-35^{o}C [1]. Operators outside of this range will have a negative impact on the performance and lifetime of the batteries. The main impacts of the improper battery temperatures are reviewed here.

2.3.1. Degrading performance

High cell temperatures lead to an increase in the cell internal resistance which will reduce the output power. In addition, higher temperatures will increase the cycle performance loss. Cycle loss is the capacity abatement of the cells when it is cycled (e.g. charged then discharged). Cells that operate at higher temperature have a higher capacity loss after each cycle in comparison will cell at lower temperatures [6].

2.3.2. Temperature distribution

As the battery packs increase in size and charge/discharge rate, more heat will be generated in them. If this heat is not dissipated properly, it will accumulate inside the battery packs. In addition to that convective heat transfer is higher at the outer surfaces of the pack. Thus, there will be uneven temperature distribution inside the battery packs. As discussed in the previous section, the performance of a cell is highly dependent on its temperature. This means that temperature maldistribution will lead to capacity variability between cells. This will create a vicious cycle where the cells with proper temperature need to deliver higher power to compensate for the low performing cells, which by itself leads to an increase in cell temperature [7]. In addition, lithium cells are low tolerance to overcharge therefore the overall charging capacity of a battery pack is limited to its lowest performing cell [8].

2.3.3. Thermal Runaway

When the cell temperature goes above a certain limit, it will allow a series of undesirable exothermic reactions to occur which will further increase the temperature. This chain type reaction will continue and lead to an incident called thermal runaway.

Feng et al. [9] performed an experimental study on prismatic 25 Ah Li-ion batteries and he recorded up to 870^{o}C internal cell temperature. The high amount of heat and gas produced during a thermal runaway can lead to fire and explosion if it is not managed properly.

Thermal runaway can occur for several reasons such as high temperature, overcharge, short-circuit and nail penetration. In this review, the focus has been on thermally caused incidents.

Thermal runaway is initiated at about 90^{o}C when the SEI (solid electrolyte interface) decomposes. SEI is the protection between the negative electrode and liquid electrolyte. With SEI damaged, the electrolyte and electrode will start reacting at around 100 ^{o}C. This reaction is highly exothermic and will further increase the temperature. At 130 ^{o}C the separator between anode and cathode melts down and causes an internal short circuit. At 200 ^{o}C a chain reaction might start, first the lithium metal oxide and then the electrolyte will react with oxygen and decompose [1].

2.4. Battery thermal management system (BTMS)

As discussed in previous sections, the inappropriate battery temperature will have a negative impact on the performance, lifetime and safety of the batteries. Therefore, a BTMS is required for every battery system. The primary duty of a BTMS is to keep the batteries in the optimum temperature range and maintain an even temperature distribution in the battery pack. Afterward, other factors such as weight, size, reliability and the cost must be taken into consideration based on the application of the battery packs.

The most common thermal management methods for battery packs are reviewed here.

2.4.1. Air cooling

Air is the most conventional way for cooling and has been used widely in various industries. Due to low heat capacity and low thermal conductivity, air might not seem to be a good cooling

medium. However, it is still an attractive cooling solution due to its simplicity and low cost [1]. Toyota Prius and Nissan Leaf are two of the most famous examples.

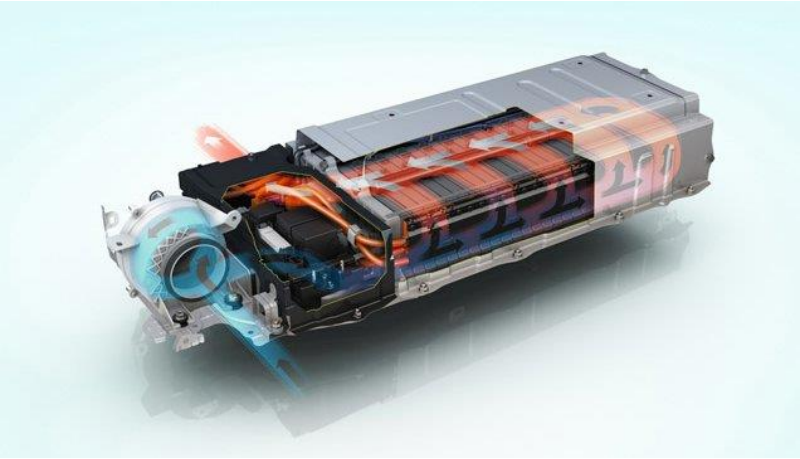

Figure 4. Toyota Prius Battery Pack with air cooling [10]

The cooling can be done by utilizing natural convection (Passive cooling) and forced convection (Active cooling). Natural convection is only suitable for low-density batteries, and typically blowers/fans are used to enhance the convection coefficient [7].

When air is used to cool a set of batteries arranged in series, its temperature raises significant due to its low heat capacity. This leads to higher cell temperatures at the pack outlet and creates an uneven temperature distribution. Thus, it is important to take extra measures to ensure the uniformity, such as Increasing the coolant medium speed, creating turbulence in the flow and optimizing the positioning of each cell. Wang et al. [11] looked at different cylindrical cell arrangement and positioning of the fan. It was found that best cooling performance is achieved when the fan is placed on top of the module and the most desired arrangement considering cooling effect and cost is when the cells are arranged side by side in a square pattern. Mahamud et al. [12] in a CFD study of cylindrical Li-ion cells showed that using reciprocating air flow can significantly improve the thermal performance of a battery module. Switching the direction of the air flow every 120s can reduce the cell temperature difference by 72% and the maximum temperature by 27%.

2.4.2. Liquid cooling

Liquid coolants have several advantages compared to air. Liquid cooling is more compact than air without sacrificing any cooling capacity. Liquid coolants can be 3500 times more efficient

than air due to higher density and heat capacity. They can save up to 40% of parasitic power compared to air cooling. In addition, liquid cooling can reduce the noise level. Nonetheless, there are downsides with liquids as well, such as cost, complexity and the leakage potential [7]. Liquid cooling can be classified into direct and indirect cooling.

I) Indirect liquid cooling

Water is used in several industrial applications as one of the most efficient coolants. However, the main challenge with directly cooling batteries with water is the short-circuit potential. Therefore, indirect methods are used to prevent electrical conduction with the cells while maintaining high thermal conductivities. Adding an electrical resistance will also add extra thermal resistance, but if it is controlled it barely affects the cooling.

The EV manufacturers, GM, and Tesla are using indirect cooling in their cars. GM uses cold plates, Figure 7, between each prismatic cell. The cold plates are thin with several microchannels passing through them. Tesla has adopted wavy tubes running between cylindrical cells, Figure 5. Thermally conductive but electrically isolating material has been used to fill the space between the cells and cooling channels. Although the wavy tubes might seem not so effective due to the small heat transfer contact area, it is safer from the mechanical and electrical point of view. All the coolant connections are made outside of the battery enclosure thus eliminating leakage points [13].

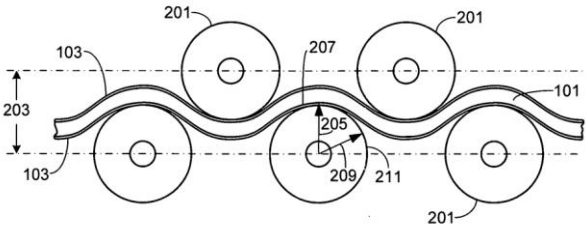

Figure 5. Tesla cooling system schematic [13]

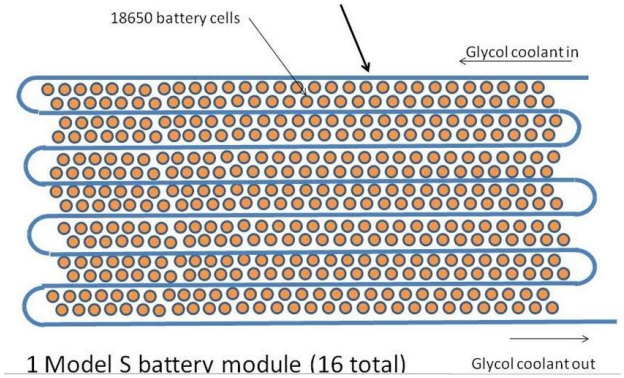

Figure 6. Tesla cooling system configuration [14]

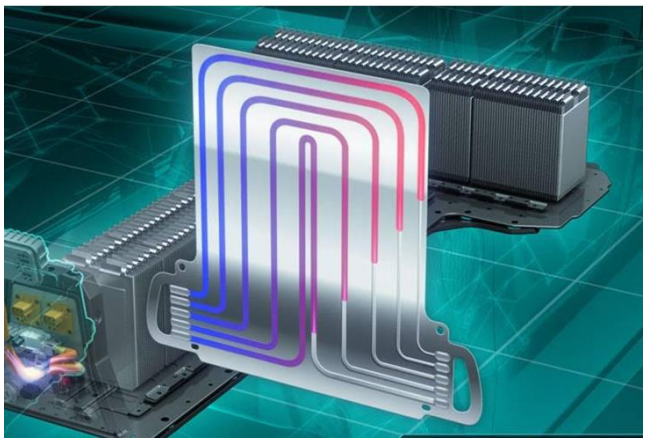

Figure 7. Chevrolet Volt Cooling system [14]

II) Direct liquid cooling (Immersion)

Direct cooling, also known as immersion cooling, covers the entire surface of the cell and cools it uniformly. This mitigates hot/cold spots in the cell and improves the performance of the cell. The coolant for direct cooling should be dielectric with low viscosity and high thermal conductivity and thermal capacity.

Immersion cooling is being increasingly used for data center servers and power electronics. Using an immersion for BTMS has still not been widely used in the mass-produced EV market. This is probably due to cost and safety concerns. As of today, to the authors' knowledge, immersion cooling for batteries has only been used for concept high performing EVs and EV racing. 3M (Minnesota Mining and Manufacturing Company) is a company that produces dielectric liquid for the cooling purpose. One example is 3M Novec 7200 Engineered Fluid [15] that is being used by Xing Mobility for Electric Racing [16]. The fluid has a boiling point of 76^{o}C which prevents the cells from reaching a higher temperature that lead to thermal runaway. They use modular containers for the cells where they will be submerged in the liquid [17].

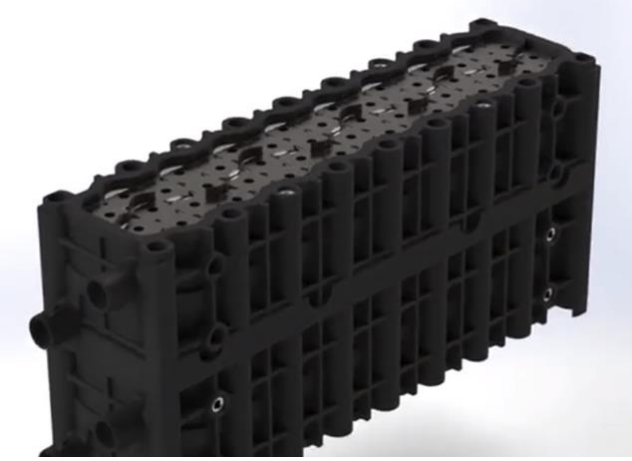

Figure 8. Xing battery module with immersion cooling [16]

Another company that uses immersion cooling technology is the electric hypercar manufacturer Rimac. They partially submerge the cells into liquid for extreme demands. Their battery pack technology is being used by other car manufacturers such as Koenigsegg's Regera [18] and Aston Martin's Valkyrie [19]. As of today, immersion cooling for BTMS has been used only for concept high performing EVs due to their high-power requirement which can only be covered by cooling. For this method to reach the mass market more improvements are needed in leakage proofing the battery pack and reducing the cost of the dielectric liquids.

2.4.3. Phase change material (PCM)

PCMs were first used for BTMS by Hallaj and Selman [20]. The phase change material has high latent heat and acts as a heat sink during battery discharge. When the cells are on standby, the PCM releases heat to the cells and the environment. The PCMs used for thermal management have a melting point in the optimum performing range of lithium cells. This way the cell temperature will stay at the right temperature for a long time.

All cells are one of the manufacturers of PCM for battery thermal management. Their product consists of paraffin (as PCM with a melting range of 32-38^{o}C) mixed with graphite flakes to enhance thermal conductivity. The graphite flakes will also create a semi matrix block which will contain the paraffin particles. Hence, even when the paraffin is melted, it stays within this matrix and the whole composition maintains its' solid form. The other advantage of solid PCM is that they also act as shields, in case one cell enters thermal runaway [21].

However, there is a downside to PCM too. If the batteries operate for a long time, or the ambient temperature is too high, then the PCM might completely melt and due to its low thermal conductivity, even act as thermal barriers. If the ambient is too cold, the PCM will add thermal mass to the modules and make it more difficult for the cells to reach the right temperature [1].

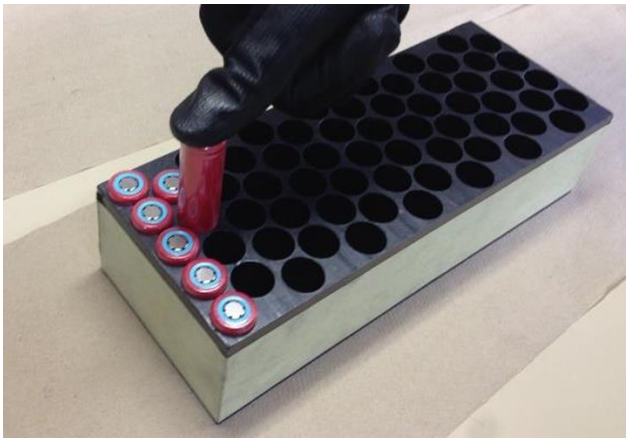

Figure 9. Battery module with PCM [21]

Overall, PCM can be the best passive solution for modules with a low operating rate or combined with active cooling (e.g. indirect liquid cooling) for higher operating rates and extreme ambient temperatures.

2.4.4. Heating

Thermal management includes both cooling and heating of the batteries. However, few studies have been done about heating. This can be due to the exothermic nature of battery operation where there will always be natural heating from the operation of the cells. Also, cooling technologies have evolved in the effort to prevent a thermal runaway which happens at elevated temperatures. While low operating temperature will only degrade the performance of the batteries, thermal runaway has catastrophic effects.

Nevertheless, in recent years with the expansion of the EV market and the significance of their range, different BTMS technologies are being investigated to optimize the performance of the EVs for cold environments. The criteria for the heating method is similar to the cooling and the time it takes to heat up the batteries in the optimum range.

Ji et al [22] studied heating of lithium cells from sub-zero up to ideal temperatures. He divides battery heating methods into three strategies, namely convective heating, self-internal heating , and mutual pulse heating.

I) Self-internal heating

At low temperatures, the internal resistance of the cells is higher, therefore more heat will be generated inside the cells as they start to operate.

II) Convective heating

The batteries themselves will supply an electric heater and a fan. The air is blown by the fan over the electric heater and the cells which warm the cells up by convective heat transfer. The convective method is the fastest way of heating.

III) Mutual pulse heating

The batteries are split into two groups. One group is discharged to charge the other group of batteries. This cycle is alternatingly repeated between the two groups. This method is faster than self-internal heating and it provides more reliable and uniform heating compared to convective heating. This method uses least battery capacity than the other two. The downside is the cost due to a more complex control system.

2.5. Battery properties measurement

Designing a safe and reliable thermal management system requires knowledge of the thermal properties of the batteries. Not accounting these properties can lead to over or under design.

As explained in section 2.1, a cylindrical lithium-ion cell consists of layers of electrodes and separator rolled into a cylinder. Due to this configuration, the cells have high conductivity along the electrode planes (axial and tangential). The radial thermal conductivity is significantly lower since the heat must pass through several layers of electrode and separator.

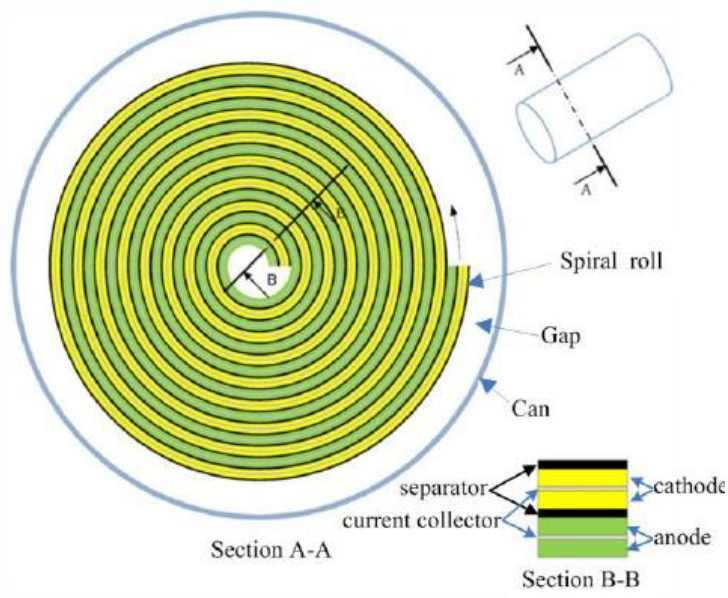

Figure 10. Configuration of the layers in cylindrical cell [22]

Measuring thermal properties of a cell are complicated, as some properties change with the state of the charge of the battery, and at the same time, it is dangerous to experiment on live battery cells. Drake et al. [23] describe a novel measurement technique for thermal conductivity and heat capacity of cylindrical lithium-ion cells using unsteady adiabatic heating. He shows that for cylindrical 18650 and 26650 $LiFePO_4$ cells the axial thermal conductivity is two orders of magnitude larger than radial thermal conductivity which was calculated to be 0,15-0,2W/m^{o}K. Spinner Et Al. [24] measured the thermal properties of lithium cells by making a surrogate cell that mimics the thermophysical behavior of a lithium cell. Axial thermal conductivity was equal to 5,1±0,6W/m^{o}K, one order of magnitude larger than radial thermal conductivity 0,12-0,197 W/m^{o}K. Ibrahim Dinçer [25] in his book about the thermal management of EVs states that the axial and radial conductivities are 25 and 1 W/m^{o}K respectively with a heat capacity of 1027 J/kg^{o}K.

3. Methodology

3.1. Model

To perform an analysis of different BTMS methods, each cooling method has been studied using Star-CCM+ software. More description of the CFD software can be found in Apendix 1, Comparison of CFD software. Models of Li-ion battery and the battery modules were made for each cooling method.

3.1.1. Lithium-ion cell

The lithium cells that are understudied in this research are of type 21700 with the following properties:

Table 1. 21700 Lithium-ion cell specification

Item	Specification*
Rated discharge capacity (1C-rate)	3,2Ah
Nominal Voltage	3,56 V
Rated Discharge energy	11,4 Wh
Density	2560 kg/m^3
Heat Capacity	1000 J/(kg*K)
Radial Thermal Conductivity	1 W/(m·K)
Axial Thermal Conductivity	25 W/(m·K)
Tangential Thermal Conductivity	25 W/(m·K)
Internal Resistace	50 mΩ

** Values provided by Northvolt*

To simplify the CFD simulation, the electrochemical reactions were not considered in the simulation. The cells are assumed as constant heat sources. The amount of heat per cell was estimated as described in section 2.2. The irreversible heat can be calculated using the internal resistance and current of the cell ($Q_{Irreversible}= I^2R$). Reversible, mixing, and phase change heat is estimated to be 20% of the reversible heat. The graph below shows the calculated total heat generated for each C-rate. C-rate is a relative measure for the performance of the battery. For

example, C-rate of one means the cell is operating at its rated capacity, C-rate of 0,5 means half of rated capacity and so on.

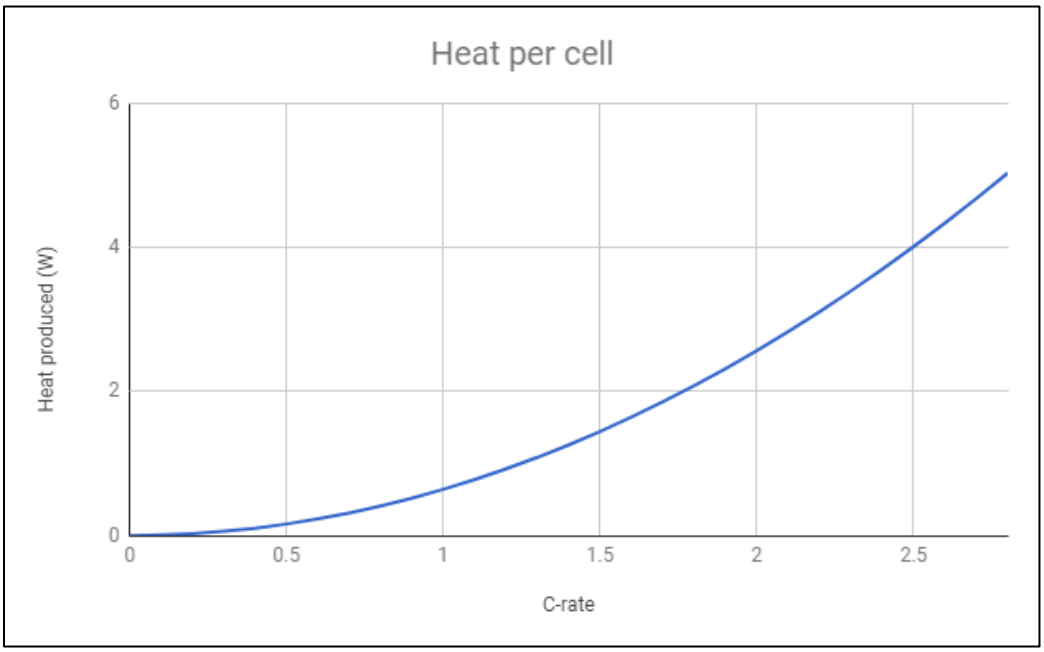

Graph 1. Heat generation in a 21700 cell

These values are used in the simulation to evaluate the performance of each cooling method for each cooling method.

3.1.2. Cooling methods

For this study, five different battery module cooling methods were chosen, namely:

- Tube cooling (Side cold plate)
- Bottom cold plate
- Air cooling
- Direct liquid cooling (Immersion)
- Solid/liquid phase change material (PCM)

The first four methods were analyzed using a conjugated heat transfer CFD simulation. The module has 96 cylindrical lithium-ion cells positioned in 6 rows of 16. Each battery cell has a height of 70mm and diameter of 21mm.

I) Tube cooling

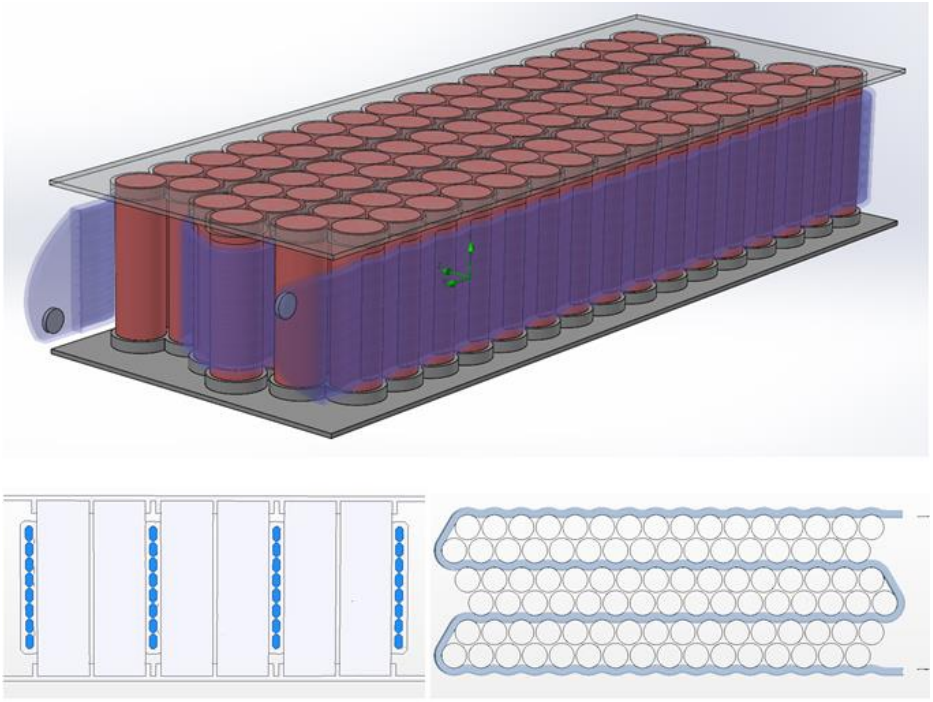

Figure 11. Geometry of tube cooling model

Figure 11 shows the geometrical model of tube cooling used in the simulation. A wave formed aluminum extrusion with 8 microchannels passes by all the cells. The coolant flowing through the microchannels is a mixture of ethylene-glycol with water (50/50% by volume). The cells are held in place with two polycarbonate clam shells (Two plates on each side with extruded rims to hold each cell in its specific place). The distance between two adjacent cells is 1,5mm (Minimum possible distance between cells provided by Northvolt).

The interface between the cells and the aluminum extrusion is filled with TIM (Thermal Interface Material) also known as gap pad or thermally conductive pad. TIM is a solid material (often wax or silicon-based) that aid heat conduction between the heat sink and the material that is being cooled. They are used to prevent air gaps on imperfect flat surfaces on a thermal contact interface [26]. This type of cooling is inspired by Tesla battery modules used in Model S and X cars [27].

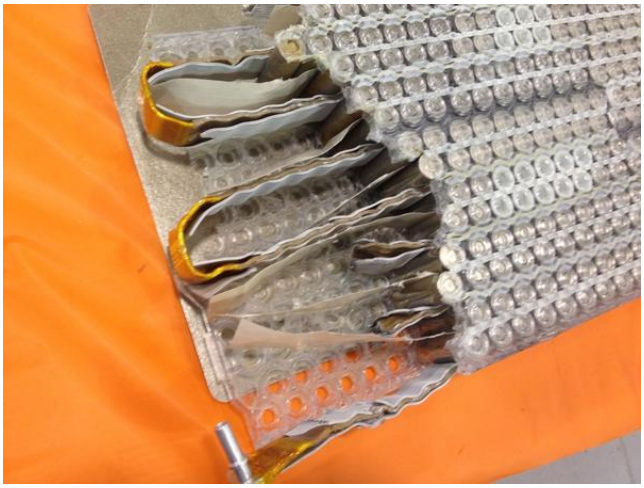

Figure 12. Tesla Model S and X battery module [28]

II) Bottom cold plate

Bottom cold plate follows the same principle as tube cooling. The cells are placed more compact relative to Tube cooling since there is no material between the cells. The advantage of this cooling method is that it takes advantage of higher axial thermal conductivity of the cells. In this model the cells are inserted 10mm into a thermally conductive polymer, thus the cold plate acts as a clamshell on the bottom of the cells as well. There are a series of channels inside, Figure 13, the plate to ensure that the coolant can flow along the plate and cool it down uniformly. The coolant used is Ethylene-glycol and water mixture like the tube cooling.

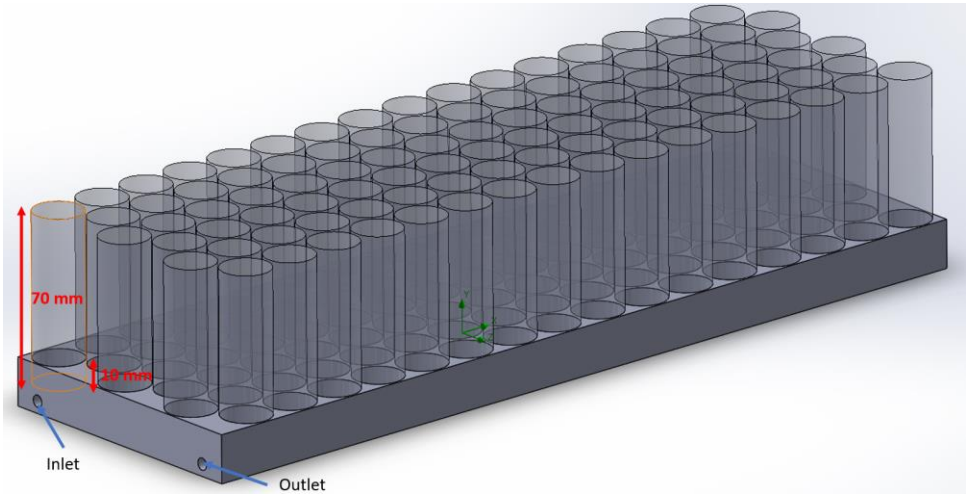

Figure 13. Geometry of bottom cold plate model

III) Air and Direct liquid cooling

The physical model used for both Air and Direct liquid cooling is the same. The cells are placed with the minimum possible distance like the previous models. The top and bottom of the cells are not considered as part of the simulation domain and the heat transfer is only going to happen for the sides of the cell. The coolant media for liquid cooling is 3M Novec 774 [29].

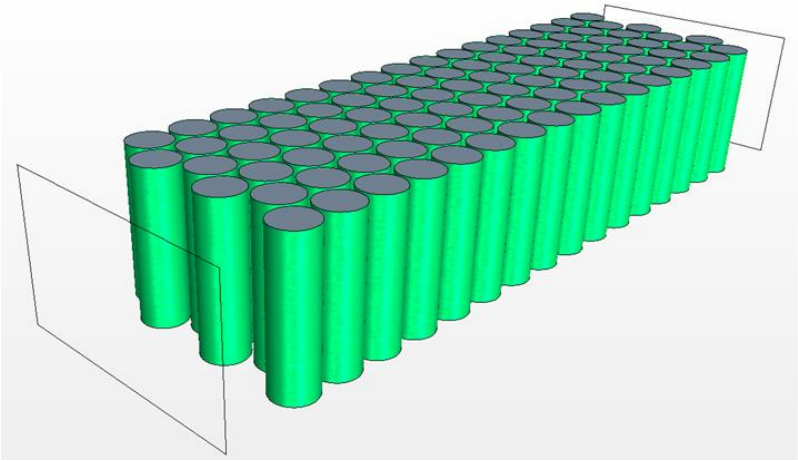

Figure 14. Geometry of air and liquid cooling model

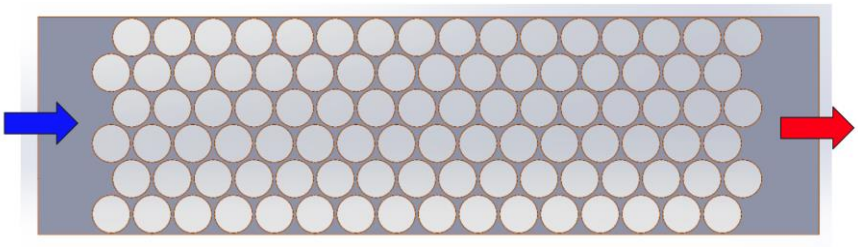

Figure 15. Liquid and air cooling model principle

IV) PCM

As it was explained in section 2.4.3, PCM are ideal for passive cooling by taking advantage of latent heat of melting. Therefore, simulation of a PCM cooling solution must consider the time variable. Since the scope of this project is limited to steady-state simulations, modeling a PCM solution would be irrelevant. Thus, this method will be investigated analytically without any CFD simulation.

3.1.3. Coolant flow

The coolant flow is set to the minimum required to keep the total coolant temperature difference between inlet and outlet equal to five degrees.

$$\frac{\dot{Q} * Number\ of\ cells}{\rho * C_p * \Delta T} = \dot{V} \quad \text{Eq. 2}$$

Q is heat generated per cell, ρ and C_p are density and heat capacity of the coolant respectively. ΔT is set to five degrees and the minimum volumetric flow of the coolant can be calculated.

3.2. Study

All the simulations are done in the steady state, as the goal has been to compare the overall performance of different cooling solutions. The results from the simulations are studied based on certain factors, namely Maximum temperature, Temperature distribution, Maximum Heat per cell, Parasitic power. In addition to these some qualitative factors such as thermal runaway protection is also discussed.

Maximum temperature: Temperature of a cell is a critical factor both for its' performance and safety. As explained in section 2.3, the maximum allowable cell temperature is 35°C. This value is recommended to have the best lifespan for cells.

Temperature distribution: As was discussed in 2.3.2, it has a direct effect on the performance of the cell. The maximum allowed temperature difference allowed between two cells and within a cell is 5 °C.

Minimum coolant required: The temperature difference in a module is directly dependent on the amount of coolant used. For each of the models, the minimum coolant needed to keep the temperature difference between cells 5 degrees is measured.

Parasitic power: The power consumed by a module cooling system affects the efficiency of it. Thus, it is important to know how much power is required for each method at different capacity rates.

4. Results and discussion

The results from the simulations are presented and discussed in the section.

4.1. Tube cooling

The first method that was analyzed is tube cooling.

4.1.1. Cell

The picture below shows the temperature distribution inside one cell running with 2W heat generation and being cooled from the tube interface. The contact interface between the cell and TIM has been set to a constant temperature of 20°C.

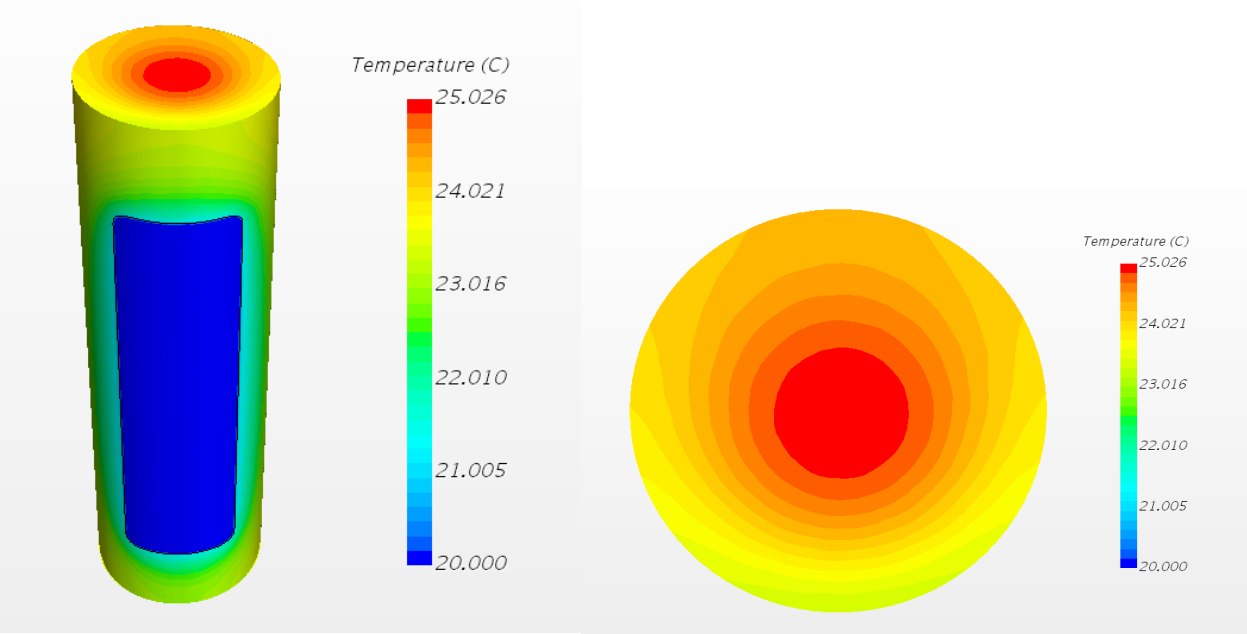

Figure 16. Temperature distribution in a cell with tube cooling

This simulation was repeated for different values of heat generation while keeping the interface temperature constant. The results are shown in the graph below.

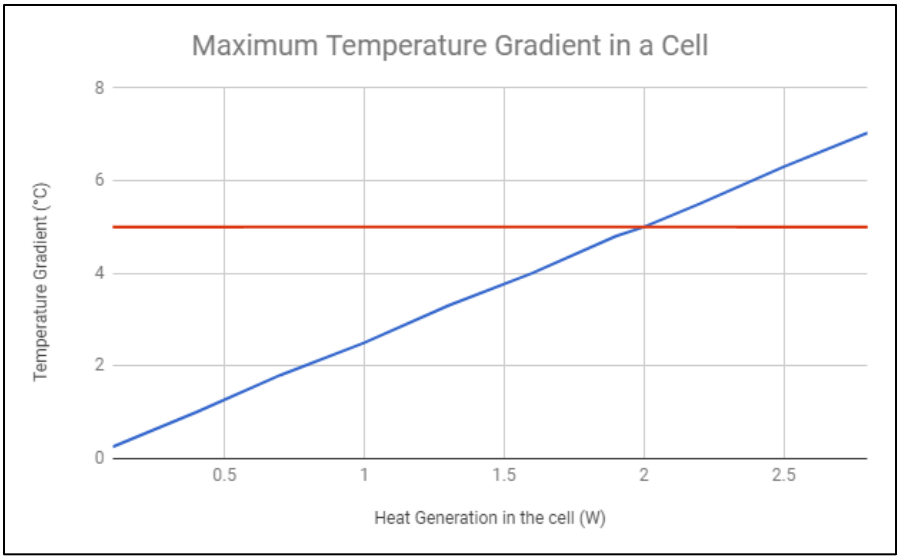

Graph 2. Maximum temperature gradient in a cell over heat generation for tube cooling

As can be seen from the graph above, the maximum heat generation at which the tube cooling system can maintain the internal temperature gradient with 5°C is 2W.

The amount of coolant flow required for each heat generated is set to the minimum flow that would keep the temperature difference of the coolant at the inlet and outlet at 5°C. Results are shown here.

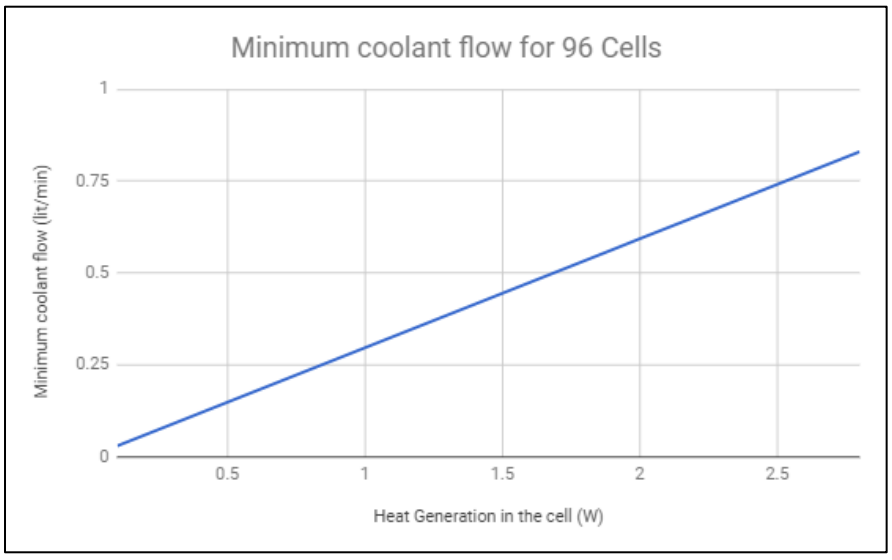

Graph 3. Minimum coolant flow required for a module with tube cooling

4.1.2. Module

Figure 17 shows the temperature distribution inside the module running at 2w heat generation per cell. As the fluid passes through channels it gets warmer from the heat generated by the cells. As a result, the cells close to the inlet are cooler than the ones at the outlet and the hottest cell is located at the end of the cooling channel. The cells that are at the bends of the cooling channel are further cooled due to the higher contact surface with the cooling channel.

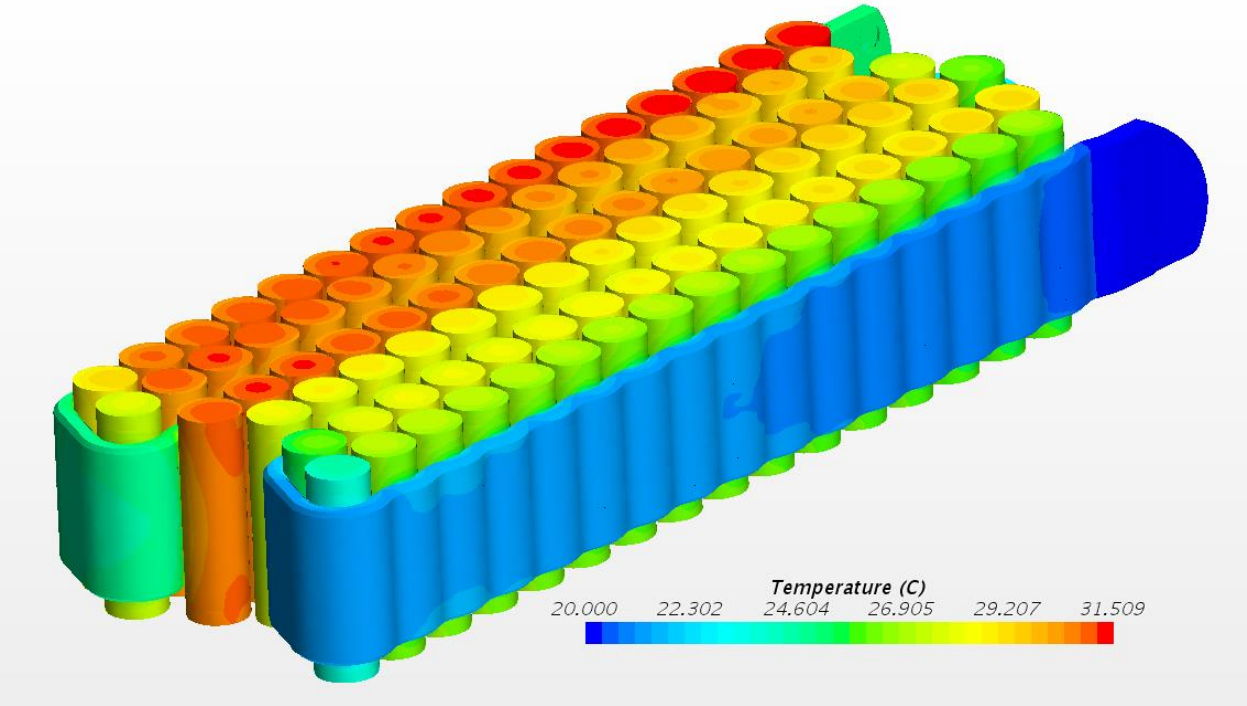

Figure 17. Temperature distribution in a module with tube cooling at 2W/Cell

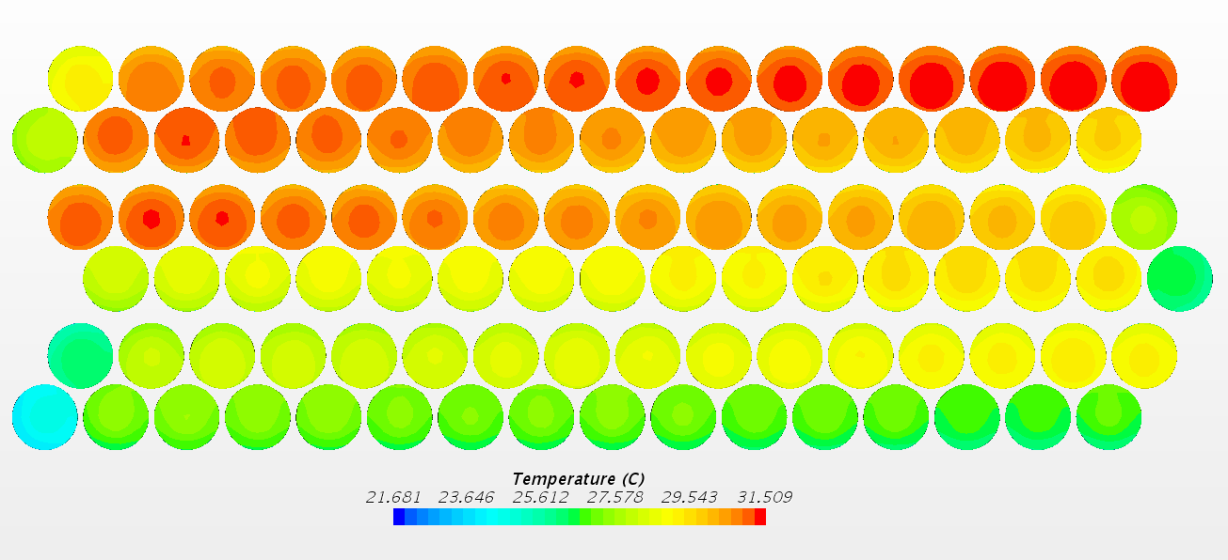

Figure 18. Horizontal temperature distribution in a module with tube cooling at 2W/Cell

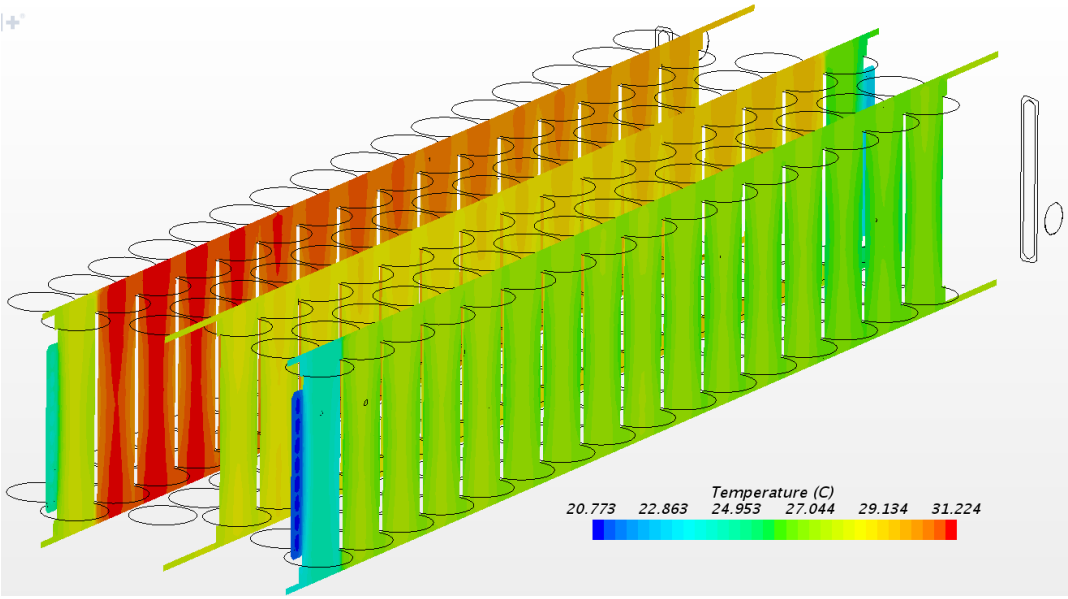

Figure 19. Vertical distribution in a module with tube cooling at 2W/Cell

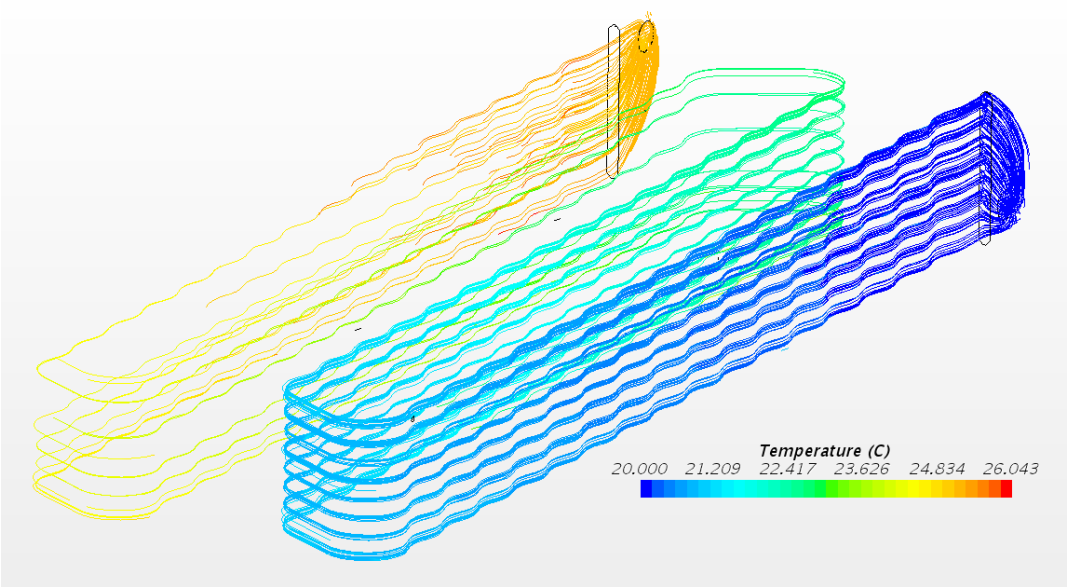

Figure 20. Coolant streamline for a module with tube cooling at 2 W/Cell

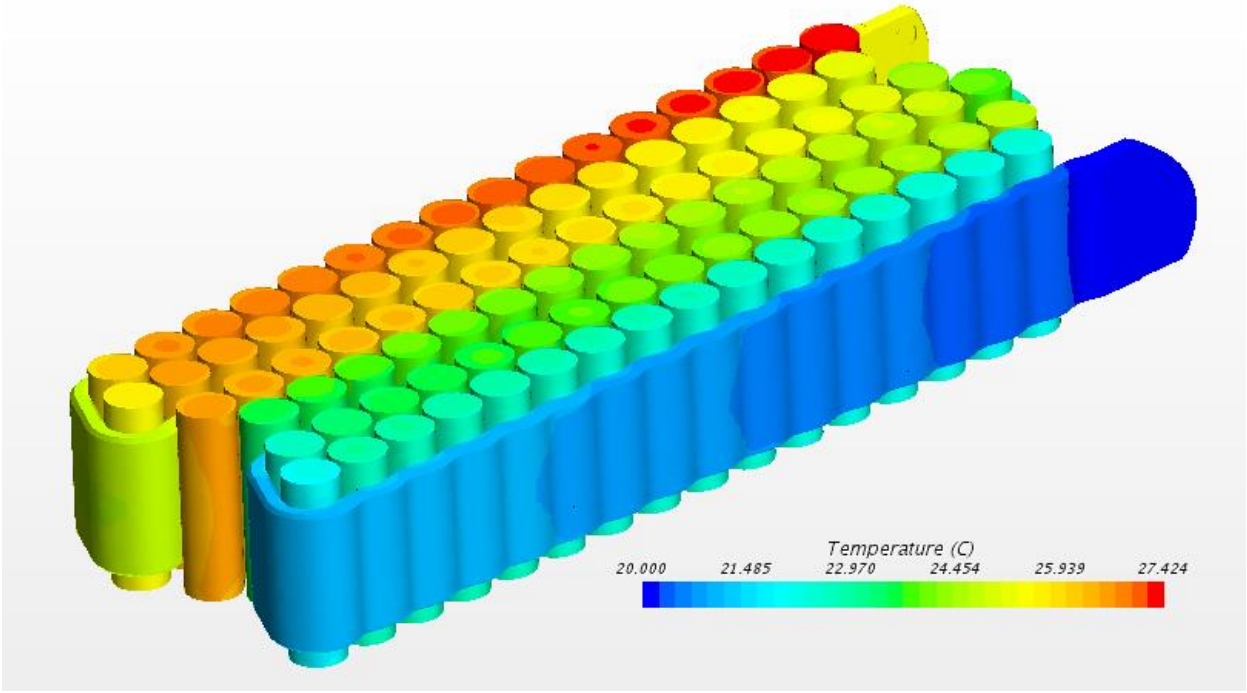

Figure 21.Temperature distribution in a module with tube cooling at 0,65 W/Cell

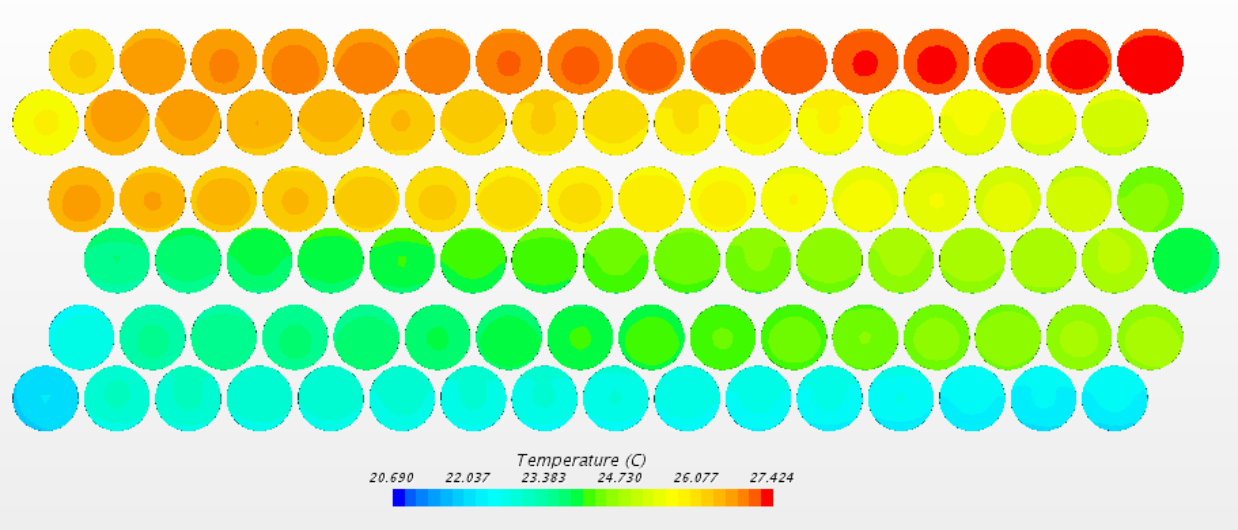

Figure 22. Horizontal temperature distribution in a module with tube cooling at 0,65 W/Cell

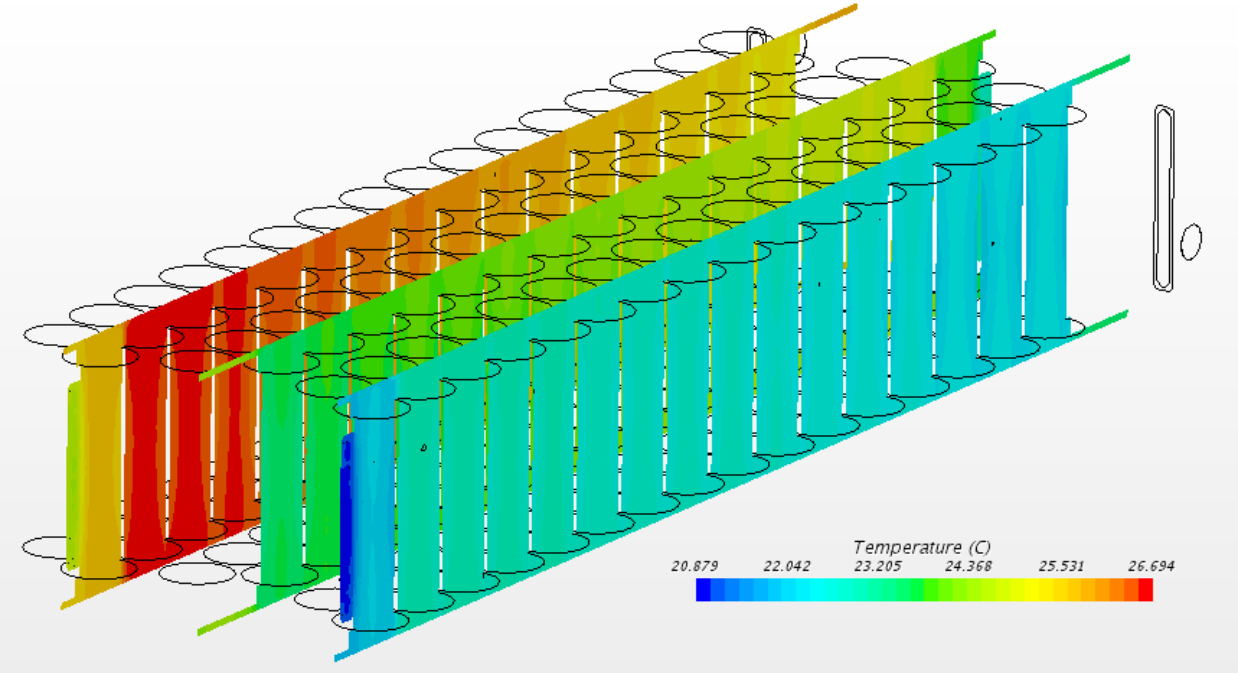

Figure 23. Vertical distribution in a module with tube cooling at 0,65 W/Cell

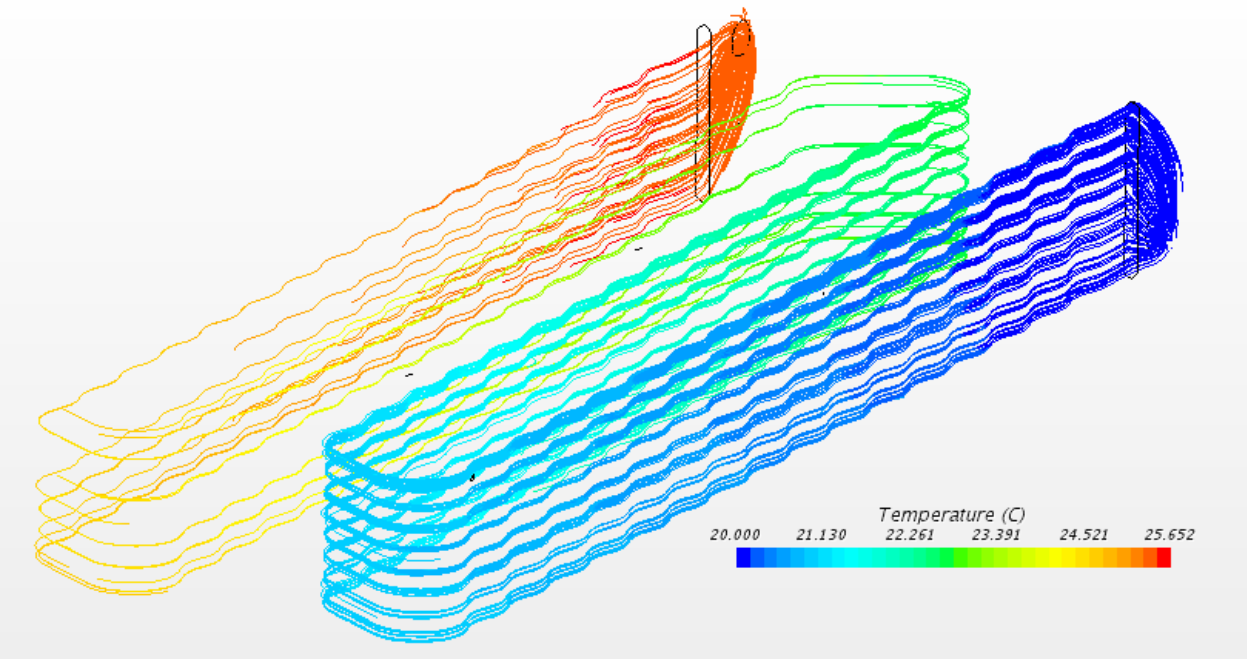

Figure 24. Coolant streamline for a module with tube cooling at 0,65 W/Cell

Table 2. Simulation results for tube cooling

Heat generation per cell (W)	**2 (Cooling limit)**	**0.65 (Equivalent to 1C)**
Coolant type	**Ethylene glycol water mix**	**Ethylene glycol water mix**
Coolant Flow (lit/min)	**0,6**	**0,19**
Coolant Temperature difference (°C)	**5,12**	**5,4**
Max temperature difference in a module(°C)	**4,53**	**5,0**
Temperature difference in a cell (°C)	**5,0**	**1,67**
Pressure difference (Pa)	**2810**	**650**
Pump power (W)	**0,026**	**0,002**

The temperature distribution within the module is relatively even with relatively low coolant flow rate and low pumping power required. The results show a small temperature distribution inside the batteries.

4.2. Bottom cold plate

4.2.1. Cell

To find the maximum cooling capability on a single cell, the bottom of it is assumed to have a constant temperature. Since heat conduction is only happening in the axial direction it can be calculated analytically based on one-dimensional heat conduction principles.

$$\frac{\partial}{\partial l}\left(k\frac{\partial T}{\partial x}\right)+\dot{q}=\rho*C_p\frac{\partial T}{\partial t}=0 \quad \textit{Eq. 3}$$

Since it is in steady state, the time factor is equal to zero. Solving the differential and rewriting the equation gives:

$$\Delta T=\frac{\dot{q}*L^2}{2*k} \quad \textit{Eq. 4}$$

Based on this, the temperature difference of 5 °C will be reached with 1,24w heat generation.

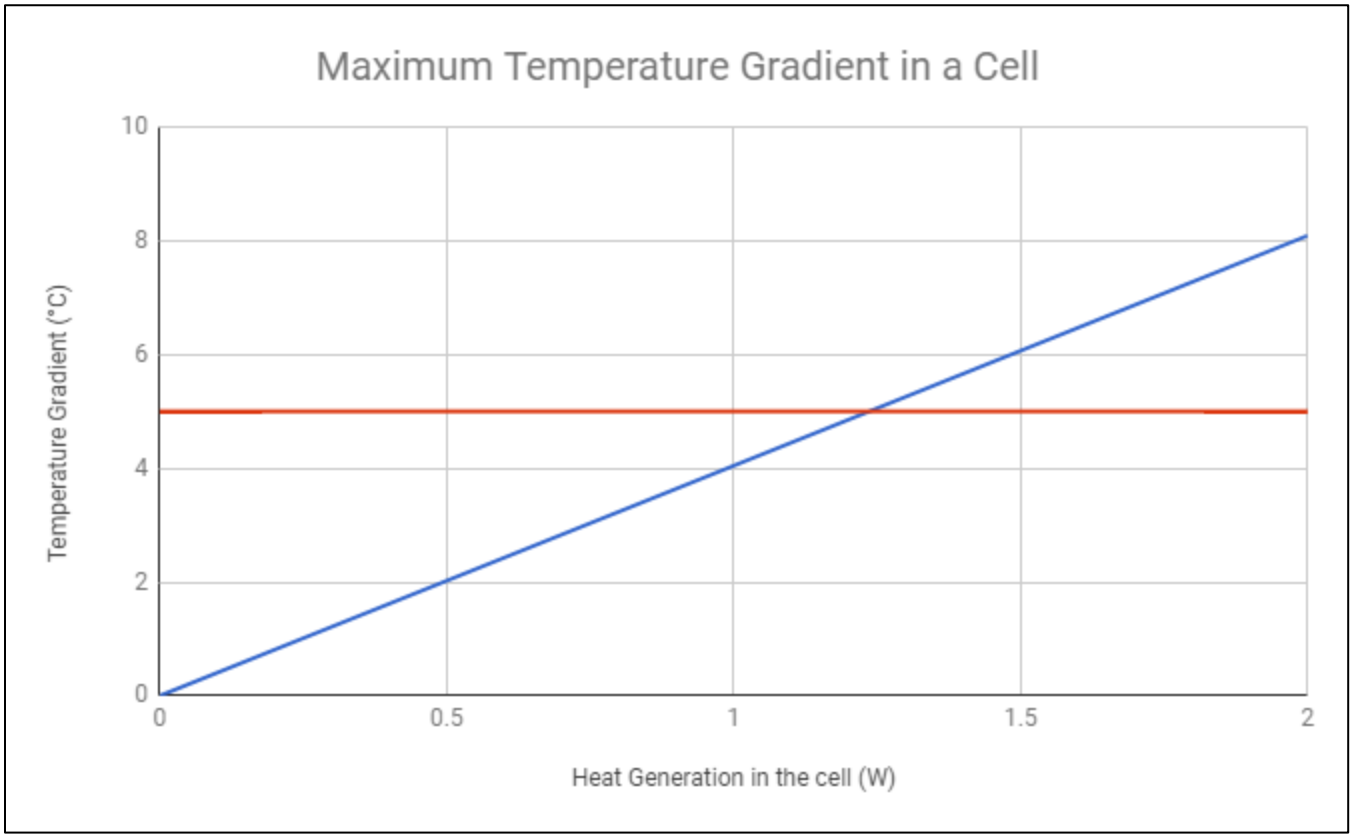

Graph 4. Maximum temperature gradient in a cell over heat generation for bottom plate cooling

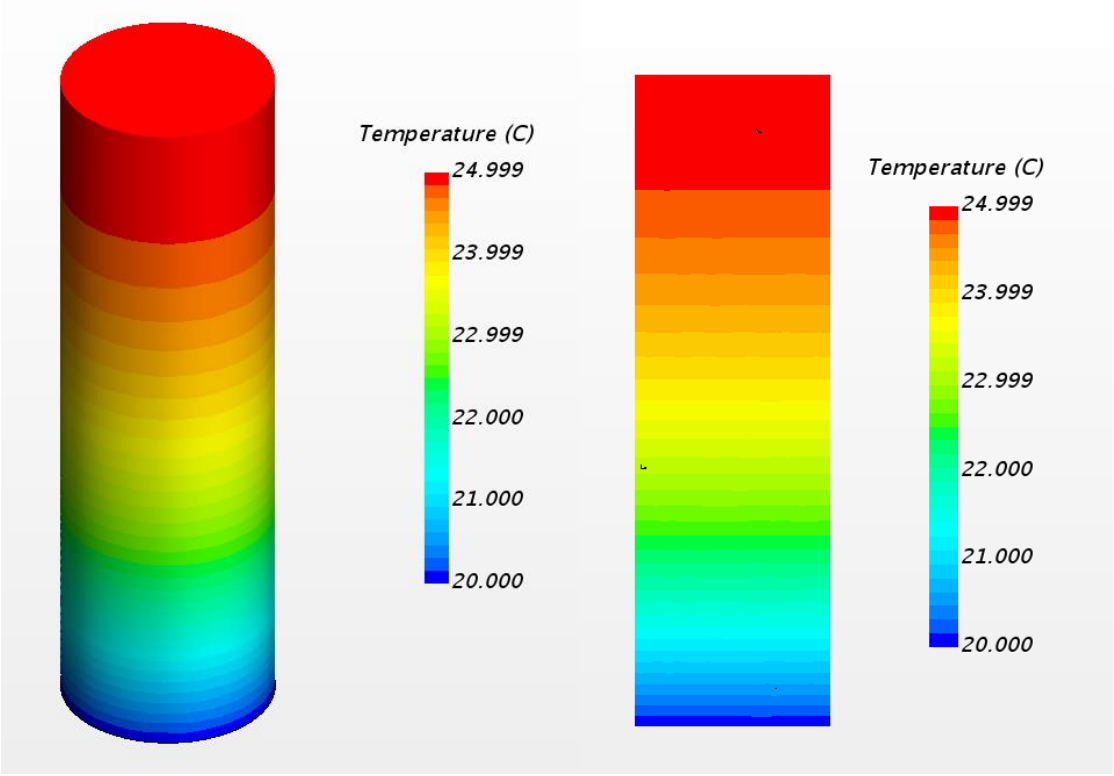

Figure 25. Temperature distribution in a cell with bottom plate cooling

4.2.2. Module

The minimum coolant flow required for the bottomed cooled module is the same as the module, which is cooling by the tubes. Here are the simulation results for a bottom cooled module. Figures below show the temperature distribution for 1,24w.

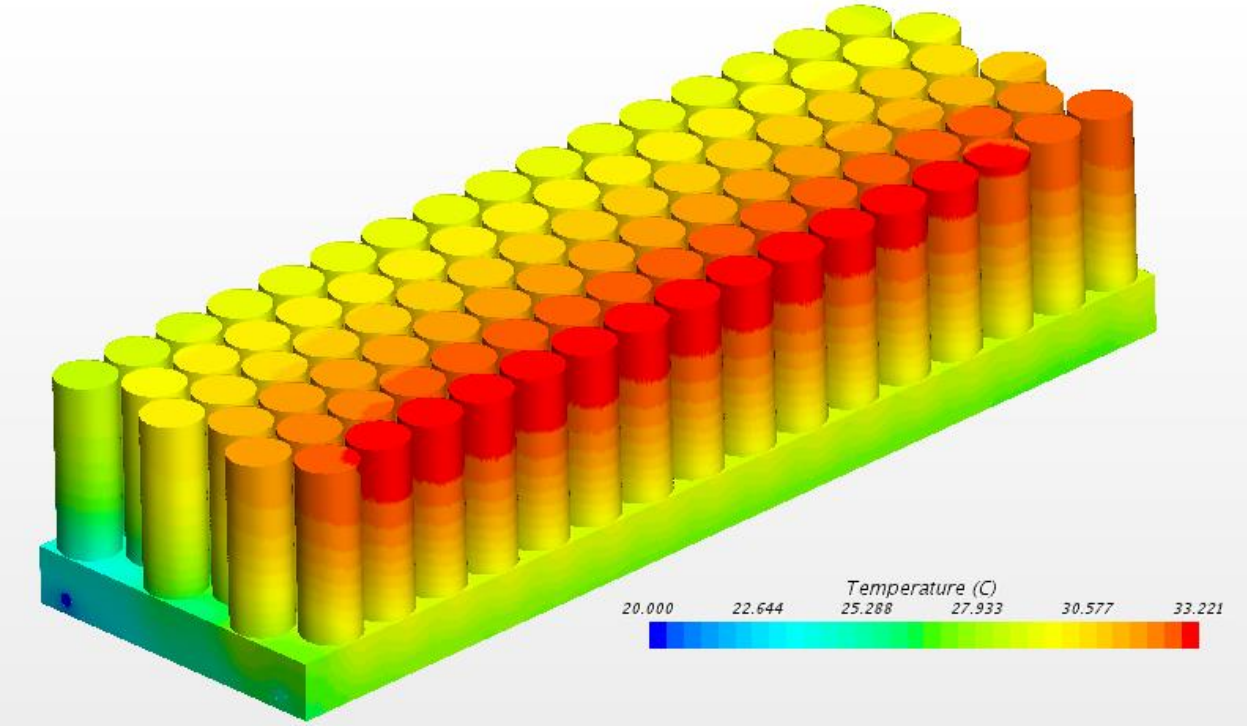

Figure 26. Temperature distribution in a module with bottom plate cooling at 1,24 W/Cell

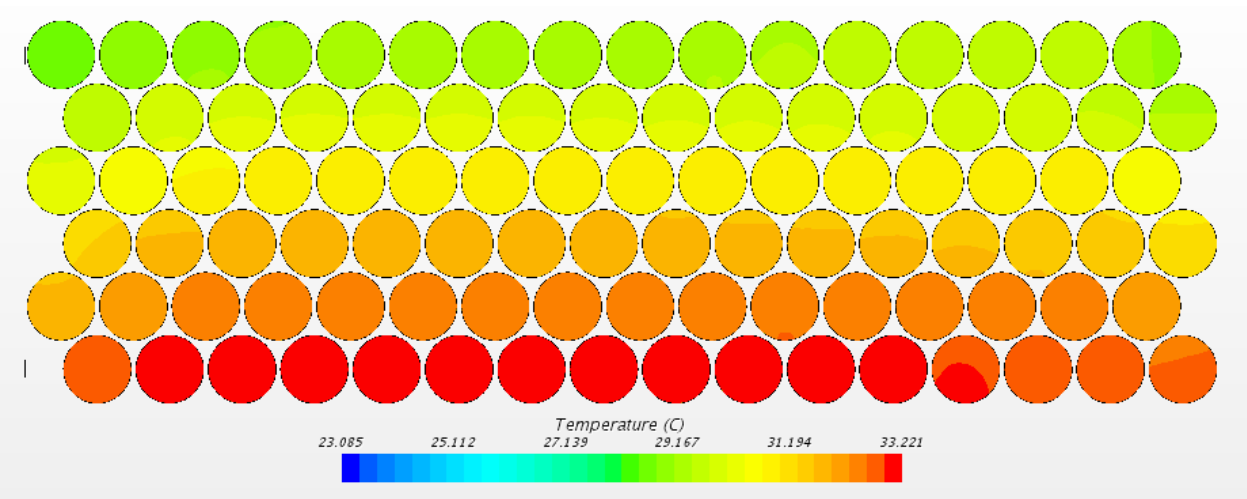

Figure 27. Horizontal temperature distribution in a module with bottom plate cooling at 1,24 W/Cell

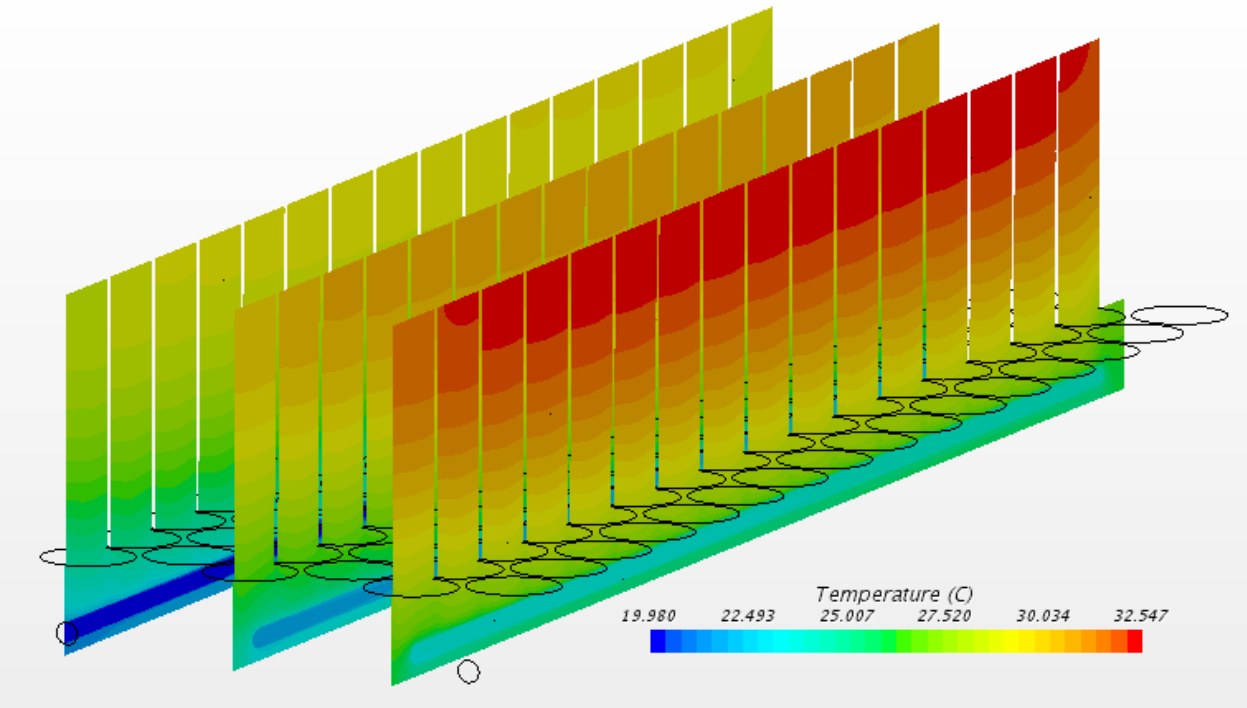

Figure 28. Vertical temperature distribution in a module with bottom plate cooling at 1,24 W/Cell

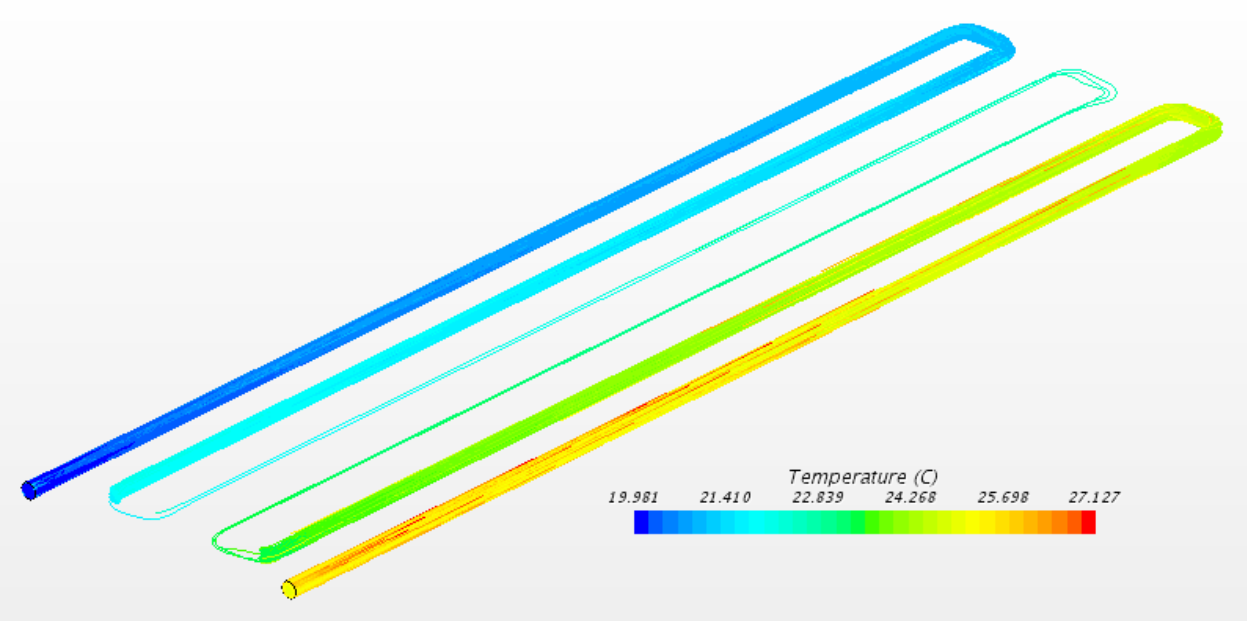

Figure 29. Coolant streamline for a module with bottom plate cooling at 1,24 W/Cell

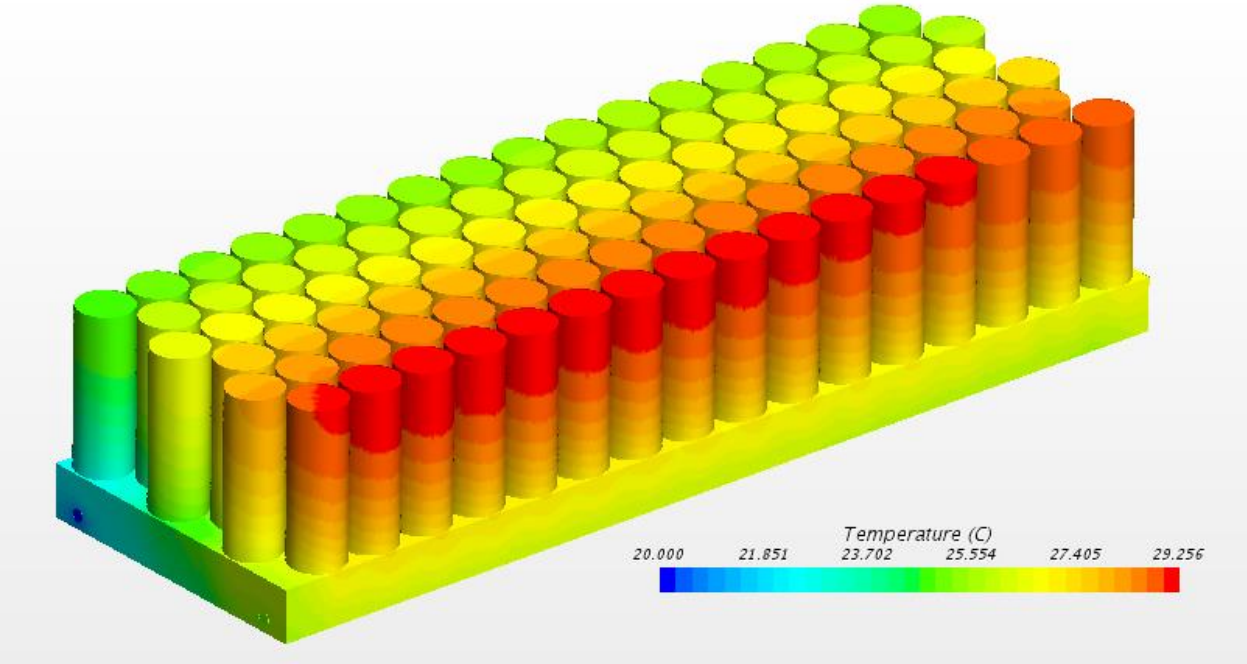

Figure 30. Temperature distribution in a module with bottom plate cooling at 0,65 W/Cell

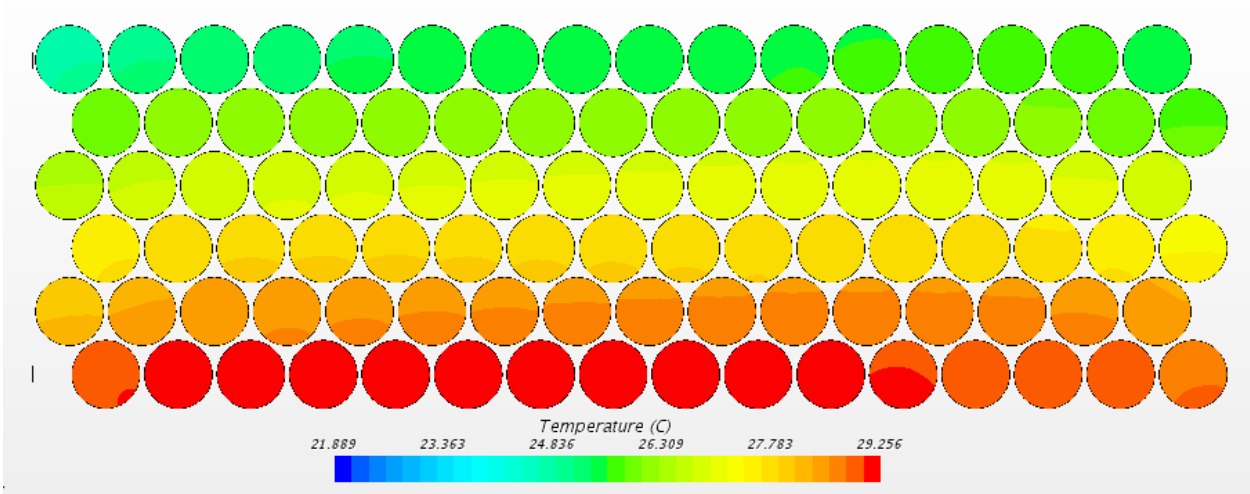

Figure 31. Horizontal temperature distribution in a module with bottom plate cooling at 0,65 W/Cell

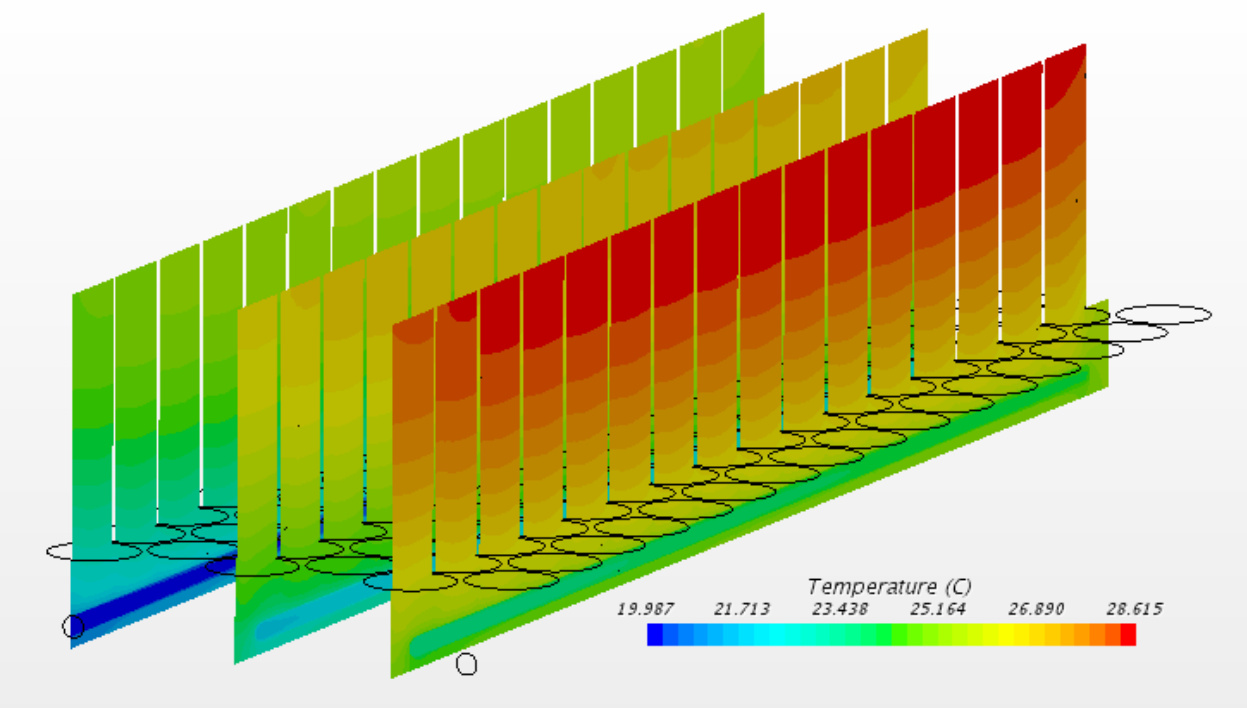

Figure 32. Vertical temperature distribution in a module with bottom plate cooling at 0,65 W/Cell

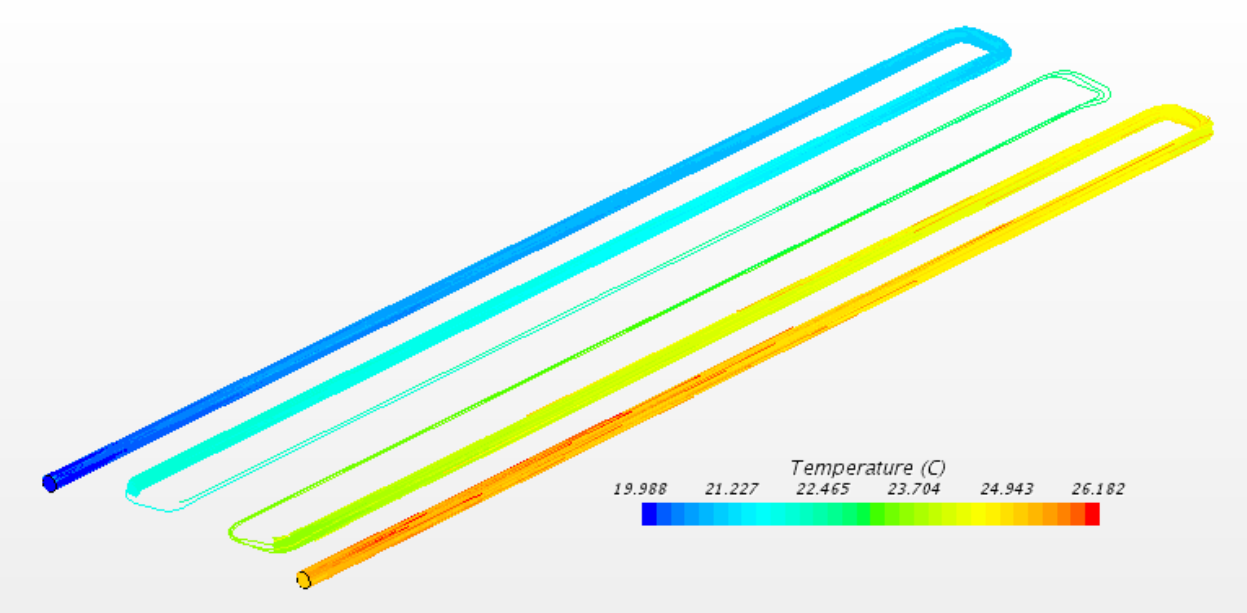

Figure 33. Coolant streamline for a module with bottom plate cooling at 0,65 W/Cell

Table 3. Simulation results for bottom cooling

Heat generation per cell (W)	**1,24 (Cooling limit)**	**0.65 (Equivalent to 1C)**
Coolant type	**Ethylene glycol water mix**	**Ethylene glycol water mix**
Coolant Flow (lit/min)	**0,37**	**0,19**
Coolant Temperature difference (°C)	**5,2**	**5,1**
Max temperature difference in a module(°C)	**4,9**	**4.9**
Temperature difference in a cell (°C)	**5,0**	**2,7**
Pressure difference (Pa)	**9000**	**4000**
Pump power (W)	**0,055**	**0.013**

The cooling method shows poor performance when it comes to the internal temperature gradient of the cells. However, the temperature distribution in a module is even.

4.3. Air cooling

4.3.1. Cell

In air cooling all sides of the cell will be cooled by air simultaneously, thus to have a theoretical limit for maximum heat generation in a cell radial heat conduction principle is used.

$$\frac{1}{r}\frac{\partial}{\partial r}\left(kr\frac{\partial T}{\partial r}\right)+\frac{1}{r^2}\frac{\partial}{\partial \emptyset}\left(k\frac{\partial T}{\partial \emptyset}\right)+\frac{\partial}{\partial z}\left(k\frac{\partial T}{\partial z}\right)+\dot{q}=\rho*C_p\frac{\partial T}{\partial t}=0 \qquad \textit{Eq. 5}$$

Since the cell is being cooled evenly from all sides, the tangential factor ($\frac{\partial T}{\partial \emptyset}$) is negligible. Same with the axial factor ($\frac{\partial T}{\partial z}$) since the cell is only being cooled from sides. it is in a steady state; the time factor is equal to zero. Solving the differential and rewriting the equation gives:

$$\Delta T=\frac{\dot{q}*r^2}{4*k} \qquad \textit{Eq. 6}$$

Based on this, the temperature difference of 5 will be reached with 4,4w heat generation. The maximum temperature gradient for each heat generation is shown in the graph below.

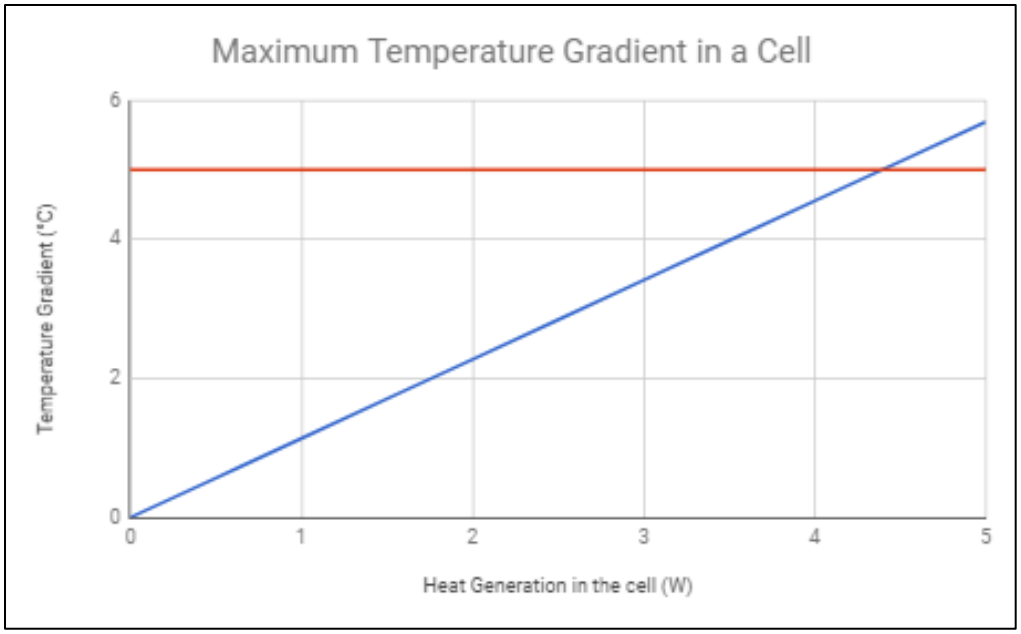

Graph 5. Maximum temperature gradient in a cell over heat generation for air and direct liquid cooling

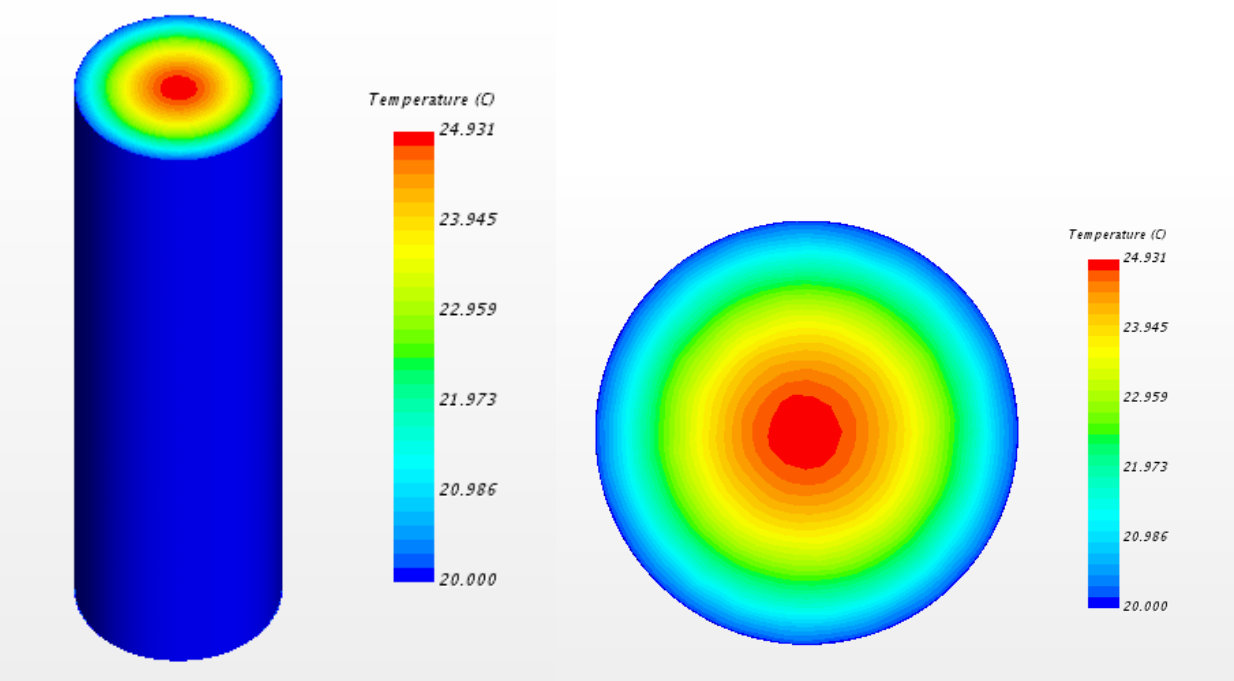

Figure 34. Temperature distribution in a cell cooled from the sides

4.3.2. Module

The amount of air needed to cool down the module and simulation results are shown below.

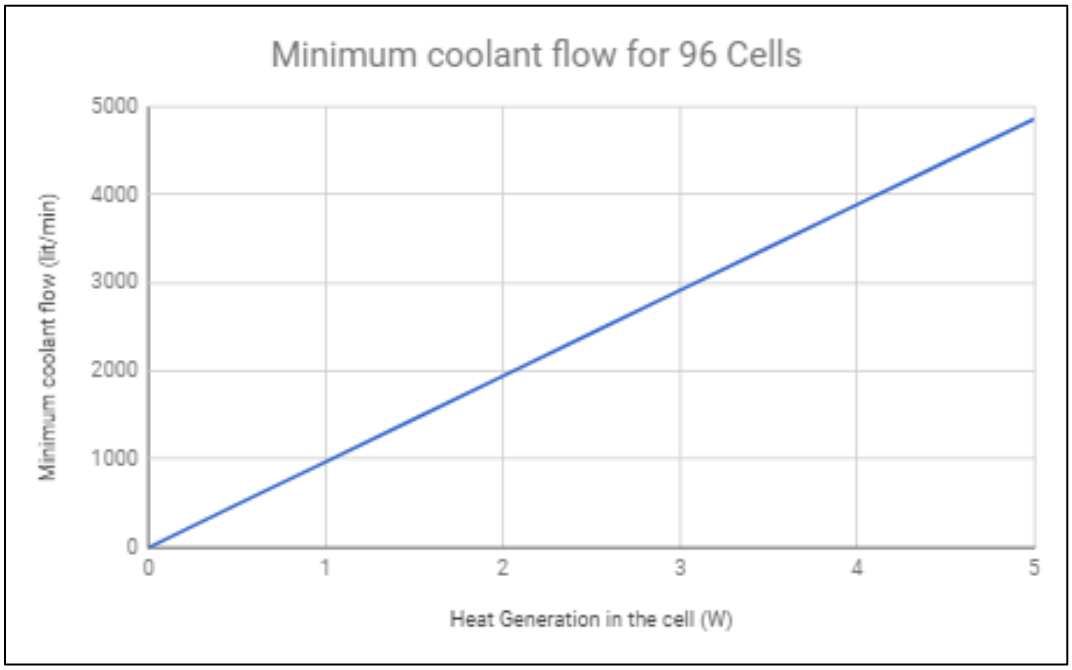

Graph 6. Minimum coolant flow required for a module with Air cooling

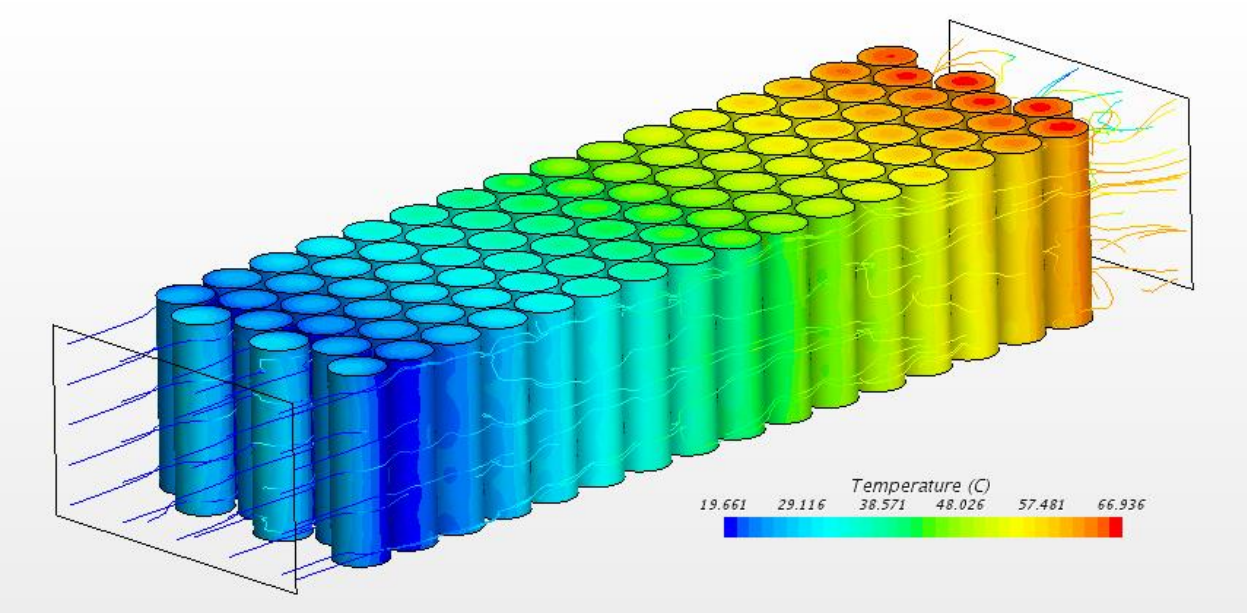

Figure 35. Temperature distribution and air flow in a module with air cooling at 4,4 W/Cell

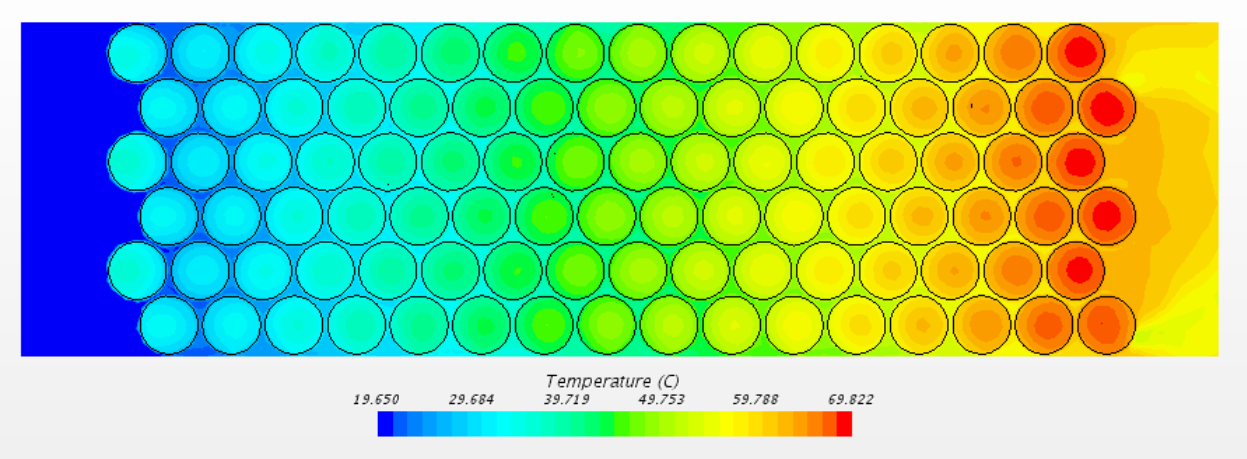

Figure 36. Horizontal temperature distribution in a module with air cooling at 4,4 W/Cell

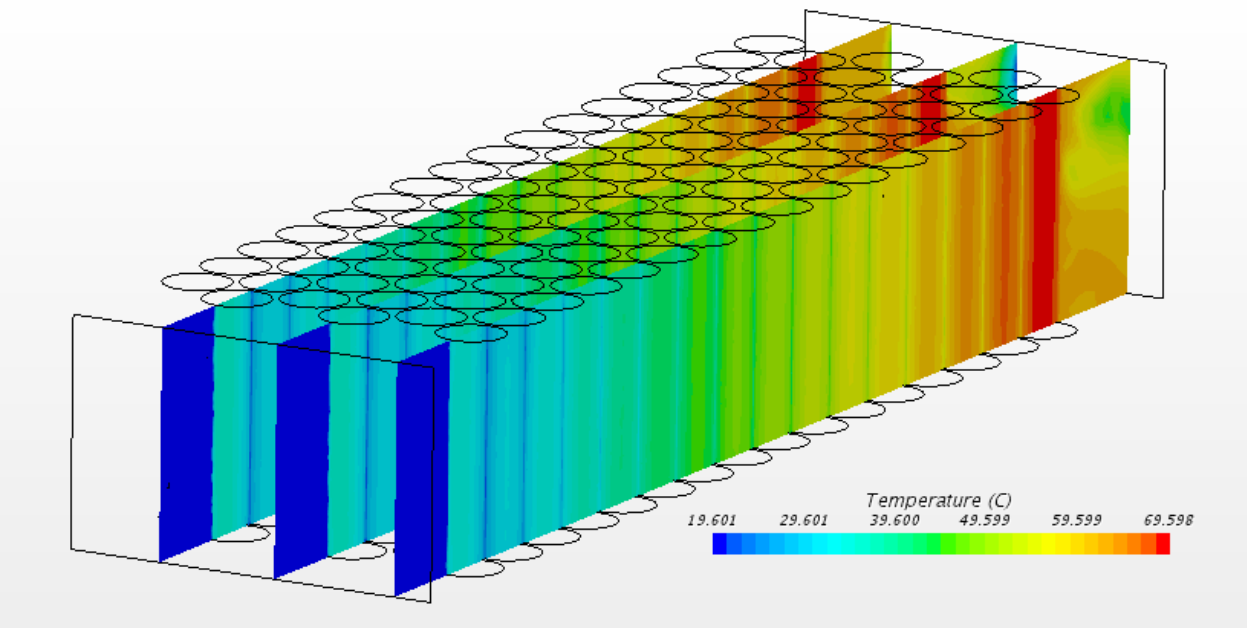

Figure 37. Vertical temperature distribution in a module with air cooling at 4,4 W/Cell

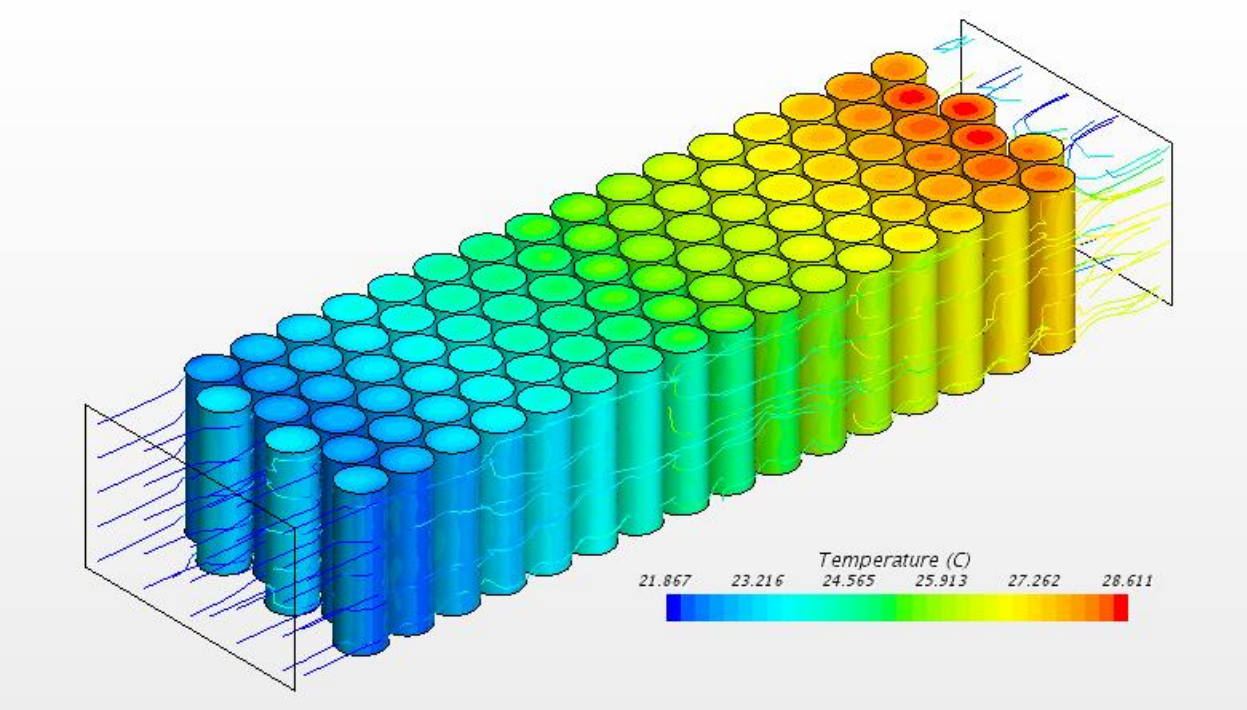

Figure 38. Temperature distribution and air flow in a module with air cooling at 0,65 W/Cell

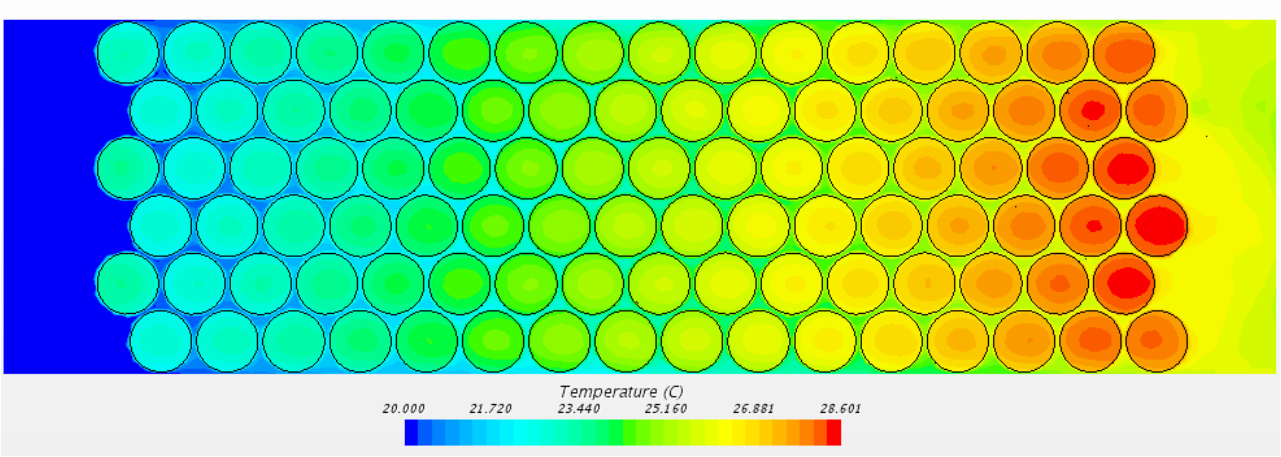

Figure 39. Horizontal temperature distribution in a module with air cooling at 0,65 W/Cell

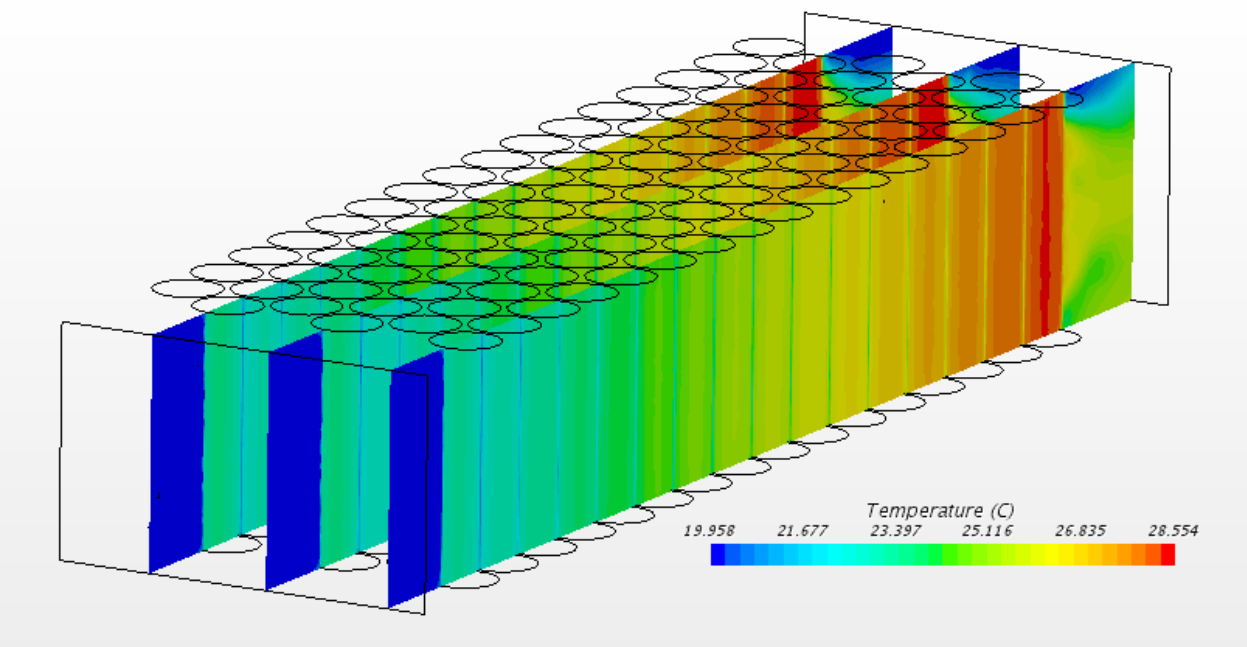

Figure 40. Vertical temperature distribution in a module with air cooling at 0,65 W/Cell

Table 4. Simulation results for air cooling

Heat generation per cell (W)	**4.4 (Cooling limit)**	**0.65 (Equivalent to 1C)**
Coolant type	**Air**	**Air**
Coolant Flow (lit/min)	**4270**	**600**
Coolant Temperature difference (°C)	**26**	**4,9**
Max temperature difference in a module(°C)	**35**	**5,2**
Temperature difference in a cell (°C)	**5**	**0,8**
Pressure difference (Pa)	**43670**	**1100**
Pump power (W)	**3110**	**11**

The temperature difference in a module is very high which is a major problem with air cooling. The amount of coolant needed, and the pumping power is significantly higher than other cooling methods which are due to the low thermal mass of air.

4.4. Direct liquid cooling

4.4.1. Cell

The analysis for cooling a single cell with direct liquid cooling follows the exact same principle as air cooling. In both cases, the cell is being cooled from the side.

4.4.2. Module

Since the cooling capacity and density of liquids is much higher than air, the amount of coolant required is much less than air cooling. 3M™ Novec™ 774Engineered Fluid [29] was chosen as the coolant since it is a non-conductive liquid and is used in the battery industry.

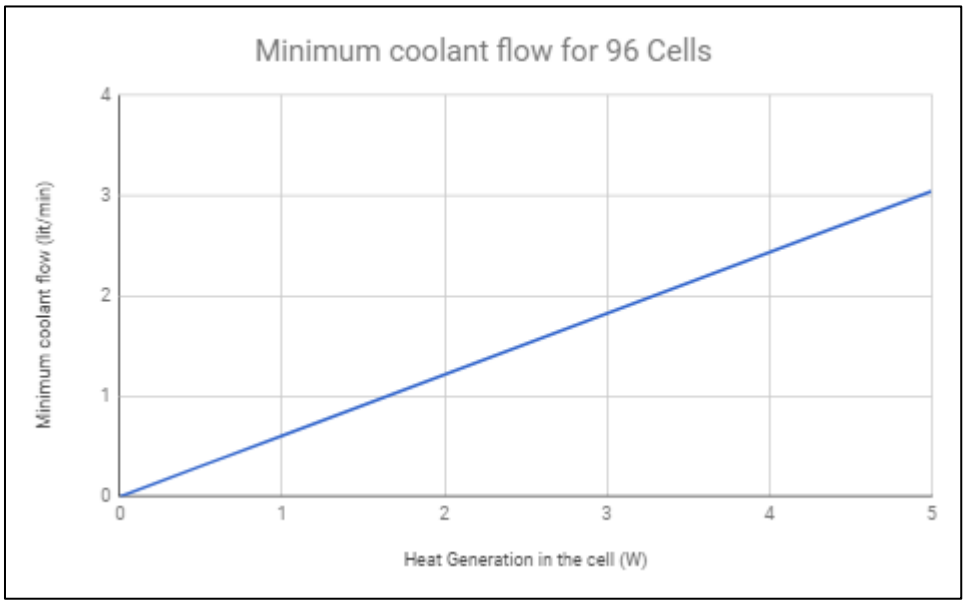

Graph 7. Minimum coolant flow required for a module with Direct liquid cooling

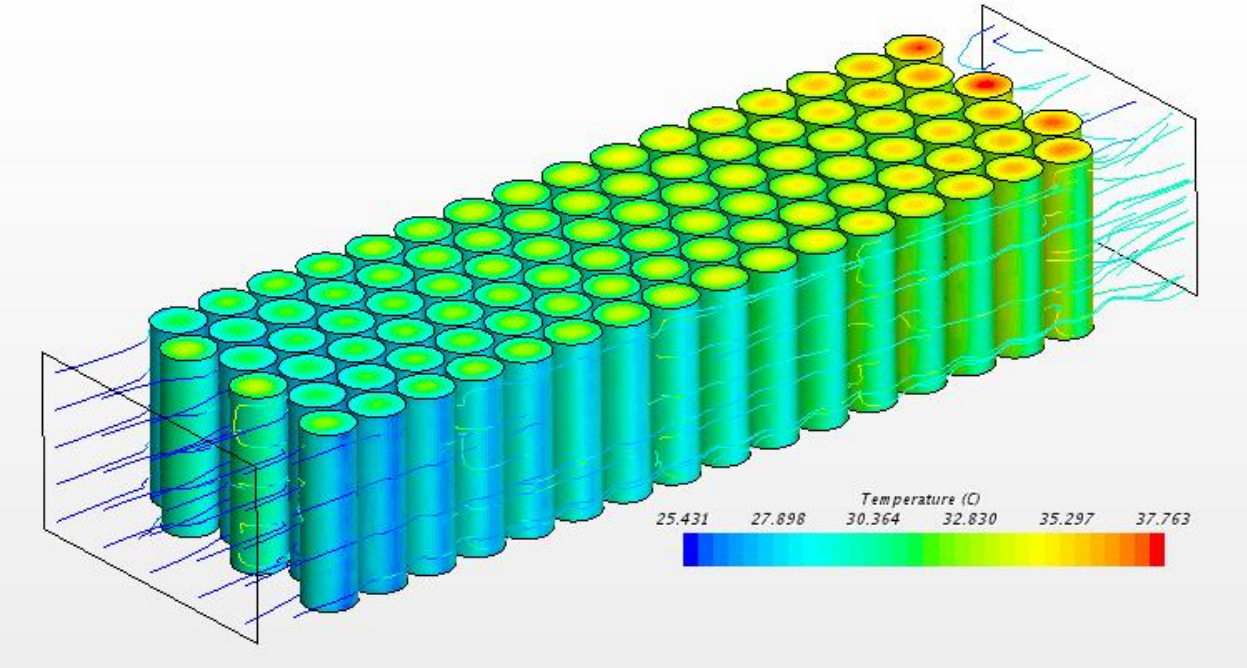

Figure 41. Temperature distribution and air flow in a module with direct liquid cooling at 4,4 W/Cell

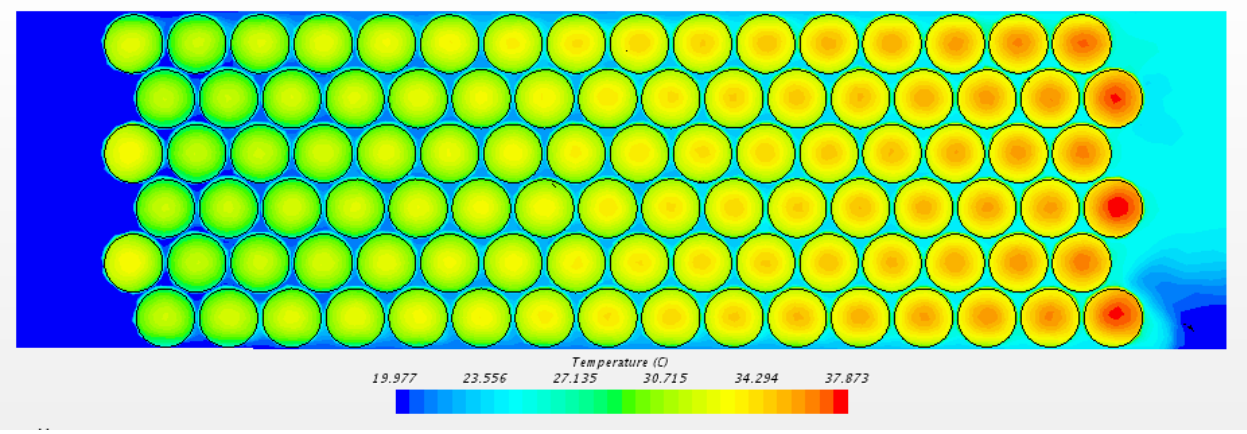

Figure 42. Horizontal temperature distribution and air flow in a module with direct liquid cooling at 4,4 W/Cell

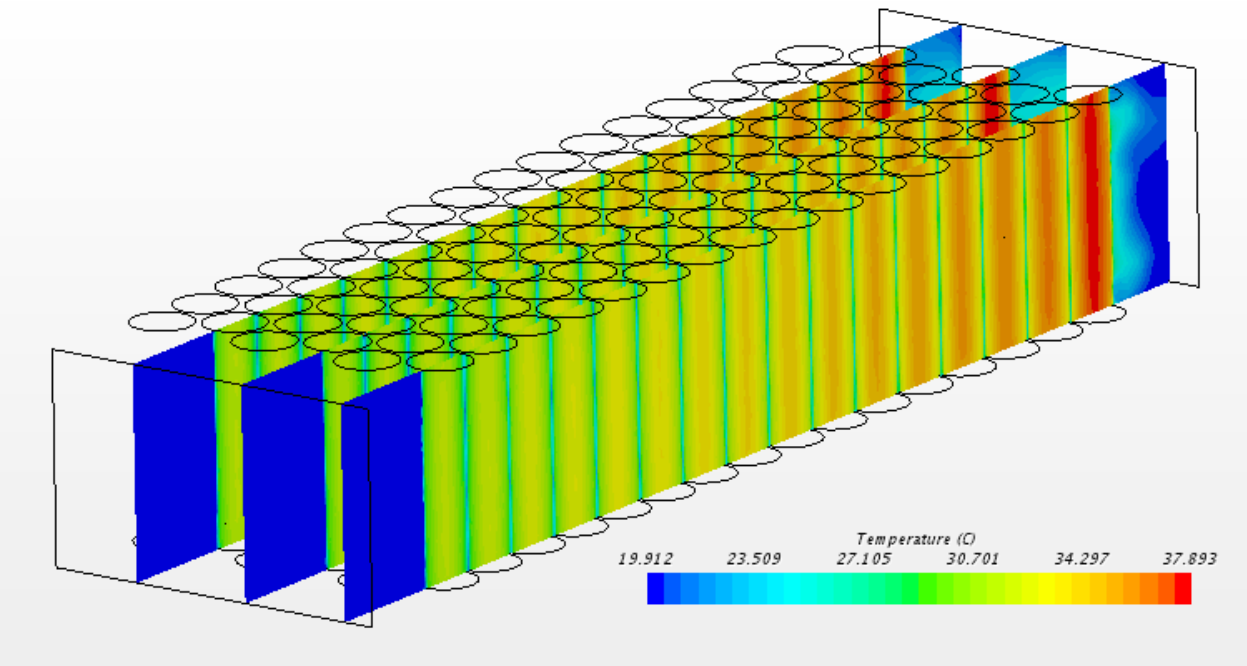

Figure 43. Vertical temperature distribution and air flow in a module with direct liquid cooling at 4,4 W/Cell

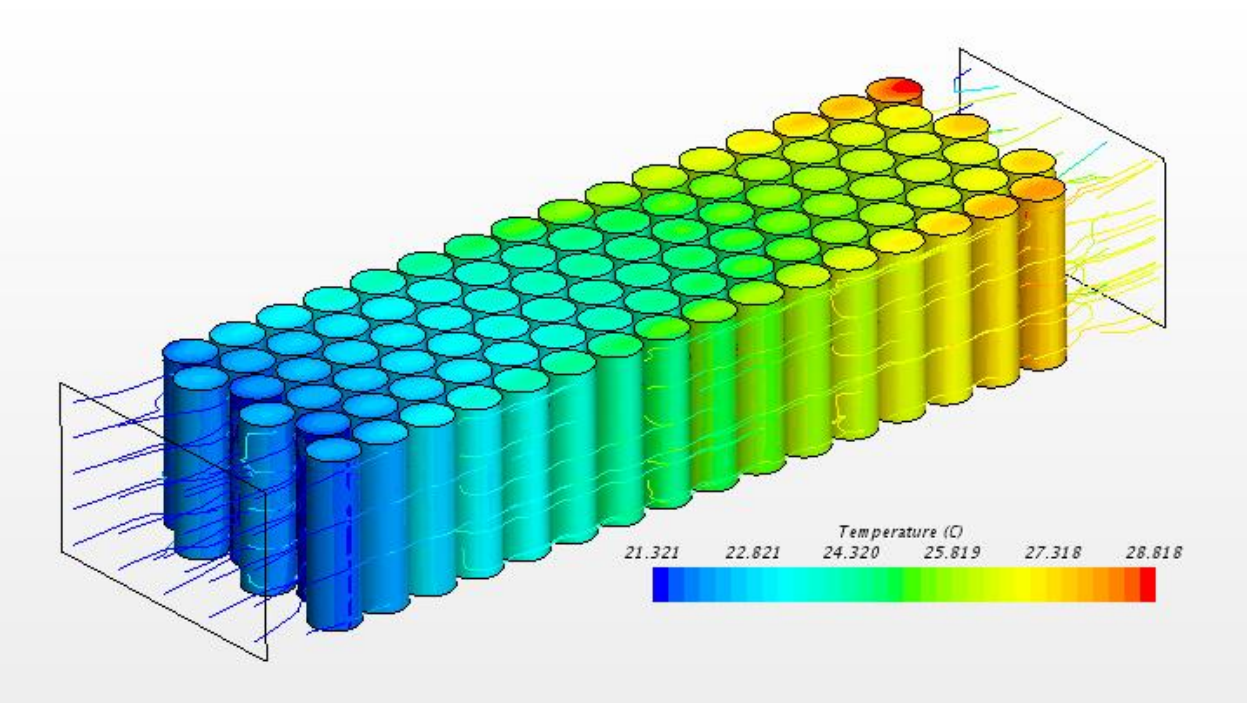

Figure 44Temperature distribution and air flow in a module with direct liquid cooling at 0,65 W/Cell

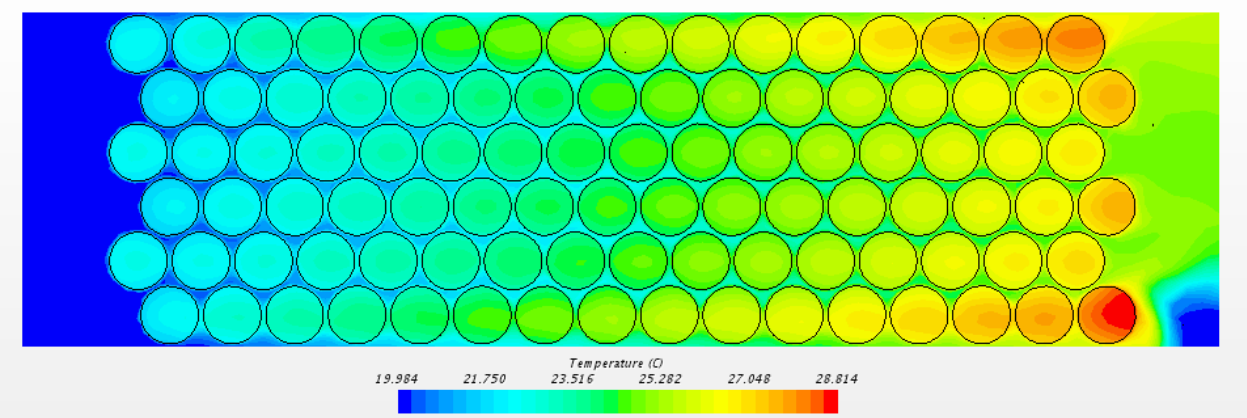

Figure 45. Horizontal temperature distribution and air flow in a module with direct liquid cooling at 0,65 W/Cell

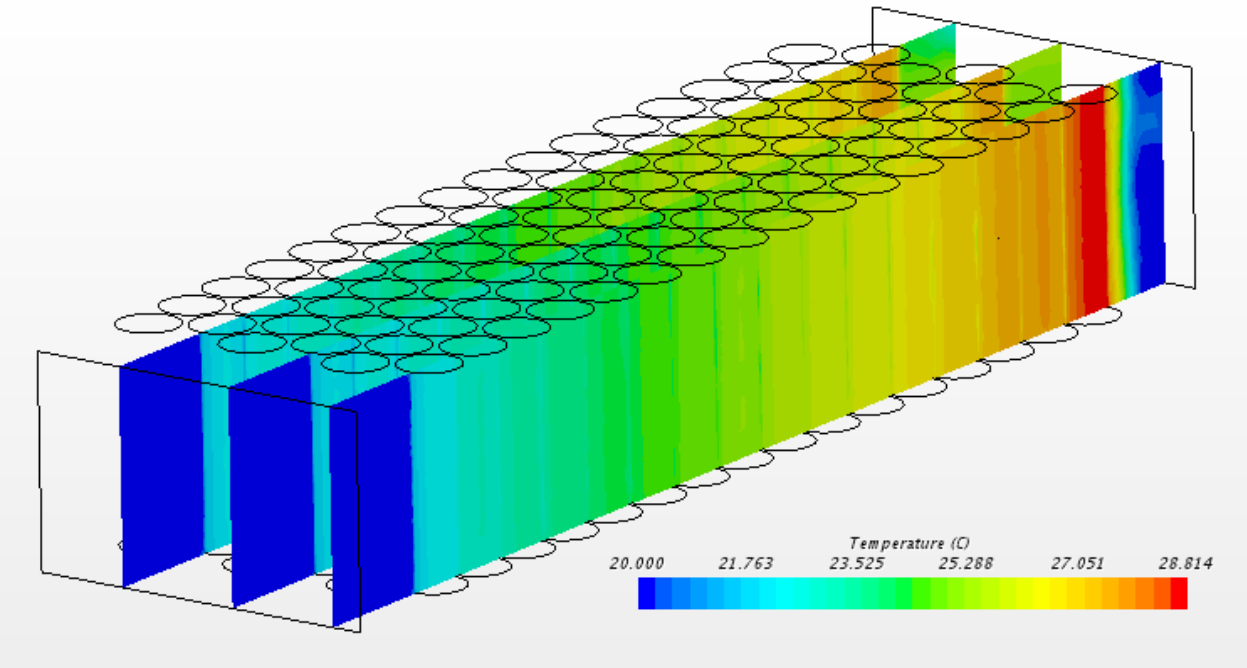

Figure 46. Vertical temperature distribution and air flow in a module with direct liquid cooling at 0,65 W/Cell

Table 5. Simulation results for direct liquid cooling

Heat generation per cell (W)	**4.4 (Cooling limit)**	**0.65 (Equivalent to 1C)**
Coolant type	**3M™ Novec™ 774 Engineered Fluid**	**3M™ Novec™ 774 Engineered Fluid**
Coolant Flow (lit/min)	**2.7**	**0.4**
Coolant Temperature difference (°C)	**6**	**6**
Max temperature difference in a module(°C)	**6**	**6**
Temperature difference in a cell (°C)	**5**	**0.8**
Pressure difference (Pa)	**53**	**4.1**
Pump power (W)	**> 0,01**	**> 0,0001**

The cells close to the outlet have a higher relatively higher temperature than the others. This is due to the turbulence created behind them which reduces the heat transfer between the cell and liquid. Otherwise, direct liquid cooling shows very good performance for high heat generations.

4.5. PCM

Normally, in a battery module, the cells are placed besides each other triangularly to minimize the space. Therefore, each cell is covered by a certain amount of PCM, which is showed by a hexagonal in the image below. The hexagonal shows the amount of PCM that is dedicated to each cell. Using the thermal properties of the cell and the PCM we analyze the temperature increase for a cell, assuming there is no cooling and temperature is distributed uniformly across the cell and PCM.

Figure 47. PCM battery module pattern

The PCM used in this analysis is Allcell PCC, see section 2.4.3, with a melting point of 37 ^{o}C. As the batteries heat up, the temperature of the module increases until they reach 37 ^{o}C and then temperature stays stagnant until all the PCM material has been melted. Afterward, the temperature starts to increase again. The figures below show the temperature evolution at 0,65w heat generation per cell for 1mm and 2mm space between the cells.

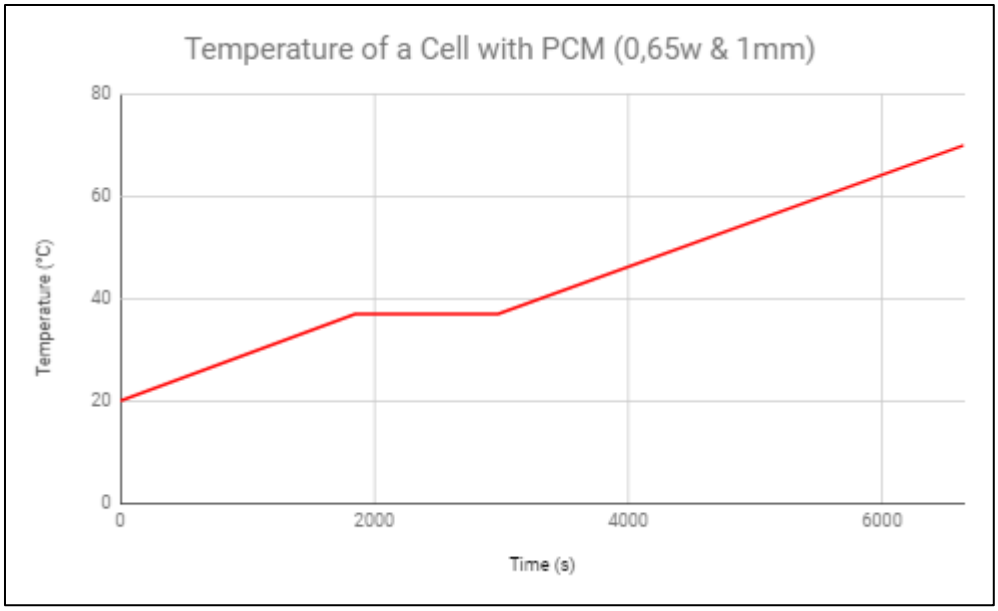

Graph 8. Temperature evolution in a PCM battery module

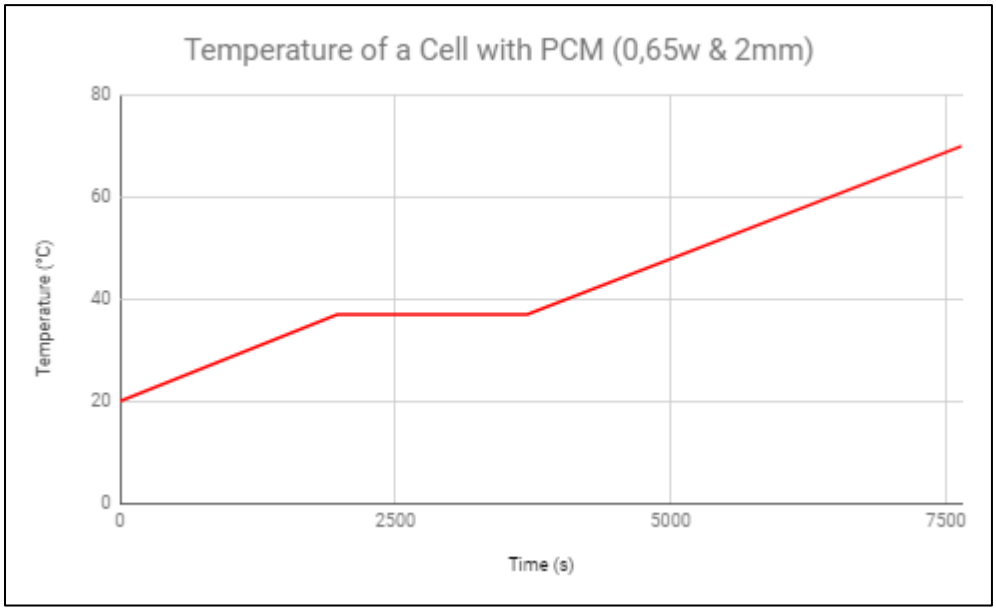

Graph 9. Temperature evolution in a PCM battery module

The effect of the PCM can clearly be seen after 1800 s. In the case with a higher distance between the cells, the stagnant temperature lasts longer since there is more material to melt as well.

5. Conclusion and future work

5.1. Conclusion

This thesis illustrates the most commonly used battery thermal management systems. One of the main contributions of this work is to present a thorough comparison of the cooling methods specific to 21700 lithium-ion cells based on CFD simulations and real industrial use cases.

A background on different battery thermal management solutions has been demonstrated, in particular, those that are more applicable in the electric vehicle and energy storage market. Four specific cooling methods have been simulated with the CFD software Star-CCM+.

The contribution of this study is twofold. First a comparison based on the literature and market research, and second new simulations for each cooling method on a battery module have been performed. Each of the methods has been simulated to find their limits and they are compared to one another based on the specific criteria used in the BTMS industry.

A glance at the results of the simulation reveals that if the coolant is in direct contact with the surface of the cell (air and direct liquid), the temperature gradient inside the cell is the lowest. Nonetheless, the disadvantage of using air cooling is the considerable pumping power and low heat capacity. It is also more challenging to have an evenly distributed cooling performance as air has a low viscosity that makes it flow less controllable.

Direct liquid cooling has the greatest cooling performance since it has the most contact surface with the cells and high heat capacity. The downside with direct liquid cooling is the complexity of the design due to its leakage potential. The non-conducting liquids required for this type of cooling are also very costly.

The indirect cooling methods (tube cooling and bottom cooling) have moderate performance. In contrast to the air cooling, the temperature distribution in the module can easily be controlled as the coolant is in thermal contact with all the cells in an identical way. The comparison between the two indirect methods shows that tube cooling induces a lower cell temperature gradient, however, bottom cooling has a simpler design.

As distinguished from the other cooling methods, phase change material is a reliable passive solution for battery modules with low power capacity. A perfect application for PCM is stationary storage systems. For higher cooling capacities, a combination of PCM and active cooling is necessary to ensure the appropriate thermal performance.

All things considered, there is simply no BTMS solution that would fit all applications. it should rather be thoroughly investigated based on the requirements, using the thermal parameters namely, the temperature gradient in a cell and a module, the maximum temperature and the required coolant flow. Furthermore, there are several external factors in choosing the right thermal management solution e.g. type of industry, use case, cost, safety, manufacturability, life-expectancy, and others.

A summary of the simulation results is presented in the image below.

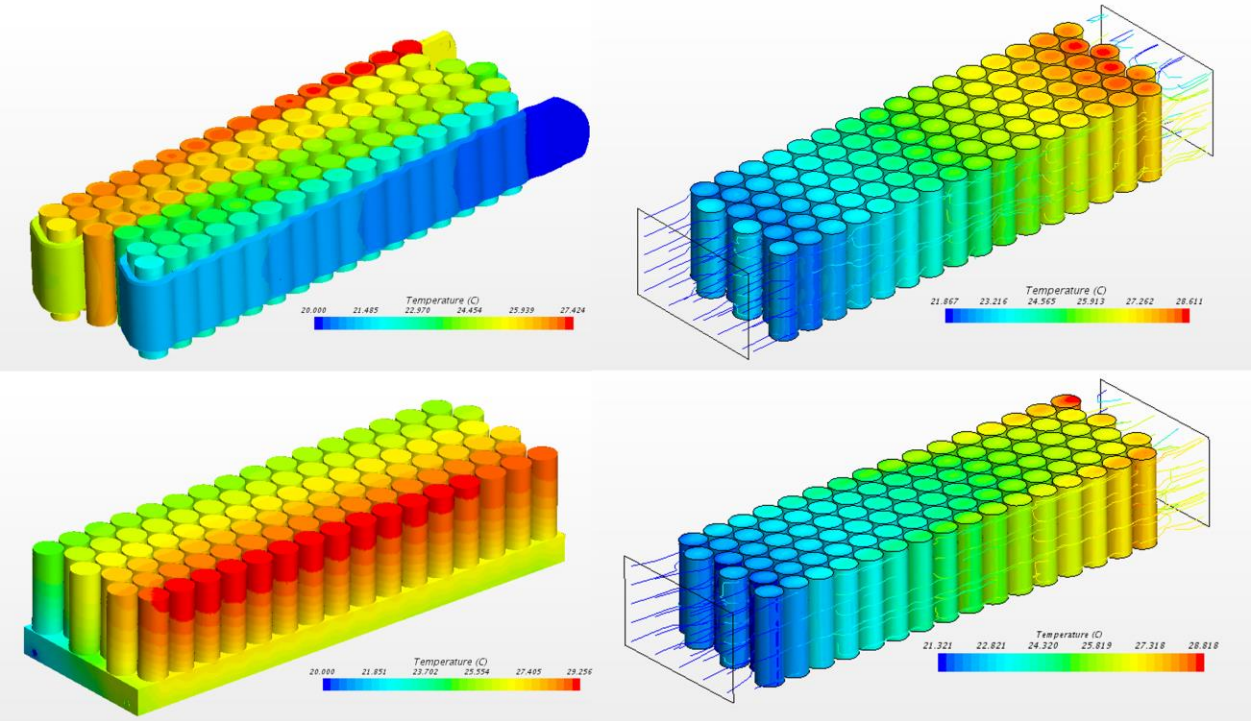

Figure 48. Temperature distribution in a module at 0,65w heat generation per cell. Air cooling (Top right),tube cooling (Top left) bottom cooling (bottom left) and direct liquid cooling (bottom right).

5.2. Future work

In this study, batteries were considered as a uniform body with constant heat generation. Even though this is a fair assumption, for a more comprehensive and case by case analysis,

parameters such as the state of charge, variable resistance, and individual battery components should be included in the CFD simulation. In addition, an actual design for an electric vehicle or energy storage application needs transient simulations based on the expected driving or load cycle. For example, the driving cycle of a fully electric car is very different from a hybrid, therefore the use case should be considered in a transient CFD model.

Obviously, as with all the simulation studies, nothing is approved until it has been tested. This thesis illustrates a good foundation for comparing different cooling methods. However, there are several parameters that might affect the outcomes when testing an actual battery system e.g. leakage, improper thermal contact, turbulence, aging, thermal runaway, and so forth.

6. Bibliography

[1] H. Liu, Z. Wei, W. He and J. Zhaoa, "Thermal issues about Li-ion batteries and recent progress in battery thermal management systems: A review," *Energy Conversion and Management 150,* pp. 304-330, 2017.

[2] R. Babcock, "EVERYTHING YOU EVER WANTED TO KNOW ABOUT LITHIUM ION BATTERIES," Vaporauthority, 23 12 2016. [Online]. Available: https://www.vaporauthority.com/blogs/news/12512333-everything-you-ever-wanted-to-know-about-lithium-ion-batteries. [Accessed 30 06 2018].

[3] B. U. Group, "BU-301a: Types of Battery Cells," Battery University, 31 07 2017. [Online]. Available: http://batteryuniversity.com/index.php/learn/article/types_of_battery_cells. [Accessed 01 07 2018].

[4] K. Onda, H. Kameyama, T. Hanamoto and Kohei, "Experimental study in heat generation behavour of small Lithium-ion secondary batteries," *Journal of The Electrochemical Society,* pp. A285-A291, 2003.

[5] T. M. Bandhauer, S. Garimella and T. F.Fuller, "A critical review of thermal issues in Lithium-ion batteries," *Journal of the Electrochemical Society,* 2011.

[6] P. Ramadass, B. Haran, R. White and B. N. Popov, "Capacity fade of Sony 18650 cells cycled at elevated temperatures, Part I. Cycling performance," *Journal of Power Sources 112,* pp. 606-613, 2002.

[7] X. Guodong, C. Lei and B. Guanglong, "A review on battery thermal management in electric vehicle applicaion," *Journal of Power Sources,* pp. 90-105, 2017.

[8] C. Kuan Cheng, C. H. Lin, S. F. Yeh, Y. H. Lin, C. S. Huang and K. C. Chen, "Cycle life analysis of series connected lithium-ion batteries with temperature difference," *Journal of Power Sources,* pp. 75-84, 2014.

[9] X. Feng, M. Fang, X. He, M. Ouyang, L. Lu, H. Wang and M. Zhang, "Thermal runaway features of large format prismatic lithium ion battery using extended volume accelerating rate calorimetry," *Journal of Power Sources,* pp. 294-301, 2014.

[10] D. Pastrascu, "Toyota Prius' Battery Recycling Plan," 2 July 2009. [Online]. Available: https://www.autoevolution.com/news/toyota-prius-battery-recycling-plan-8360.html. [Accessed 14 09 2018].

[11] T. Wang, K. Tseng, J. Zhao and Z. Wei, "Thermal investigation of lithium-ion battery module with different cell arrangement structures and forced air-cooling strategies," *Applied Energy 134,* pp. 229-238, 2014.

[12] C. P. Rajib Mahamud, "Reciprocating air flow for Li-ion battery thermal management to improve temperature uniformity," *Journal of Power Sources 196,* p. 5685–5696, 2011.

[13] Hermann and W. Arthur, "Liquid cooling manifold with multi-function thermal interface". US Patent US20100104938A1, 12 01 2010.

[14] G. Bower and K. Ritter, "Chevy Bolt 200 Mile EV Battery Cooling and Gearbox Details," 18 Jan 2016. [Online]. Available: https://insideevs.com/chevy-bolt-200-mile-ev-battery-cooling-and-gearbox-details-bower/.

[15] 3M, Electronics Markets Materials Division, "3M™ Novec™ 7200 Engineered Fluid," 9 9 2009. [Online]. Available: https://multimedia.3m.com/mws/media/199819O/3mtm-novectm-7200-engineered-fluid.pdf.

[16] XING Mobility™ Inc, "Xing modular battery system," 2017. [Online]. Available: https://www.xingmobility.com/xing-battery-system.

[17] C. Morris, "XING Mobility's electric supercar uses novel battery cooling system," Chargedevs, 01 12 2017. [Online]. Available: https://chargedevs.com/newswire/xing-mobilitys-electric-supercar-uses-novel-battery-cooling-system/. [Accessed 27 55 2018].

[18] Rimac, "RIMAC HELPS BRING WORLD'S MOST POWERFUL PRODUCTION CAR TO REALITY," Rimac-automobili, 3 3 2015. [Online]. Available: http://www.rimac-automobili.com/en/press/releases/rimac-helps-bring-world-s-most-powerful-production-car-to-reality/. [Accessed 27 5 2018].

[19] F. Lambert, "Aston Martin's upcoming new hypercar will have a battery pack supplied by Rimac," Electrek, 16 2 2017. [Online]. Available: https://electrek.co/2017/02/16/aston-martin-hypercar-electric-battery-pack-rimac/. [Accessed 27 5 2018].

[20] Selman, S. A. Hallaj and J. Robert, "Thermal management of battery systems". US Patent US6468689B1, 29 02 2000.

[21] AllCell, "Allcelltech," Allcelltech, [Online]. Available: http://www.allcelltech.com/index.php/technology/pcc-thermal-management. [Accessed 27 05 2018].

[22] Y. Ji and C. Y. Wang, "Heating strategies for Li-ion batteries operated from subzero temperatures," *Electrochimica Acta,* vol. 107, pp. 664-674, 2013.

[23] S. Drake, D. Wetz, J. Ostanek, S. Miller, J. Heinzel and A. Jaina, "Measurement of anisotropic thermophysical properties of cylindrical Li-ion cells," *Journal of Power Sources,* pp. 298-304, 2014.

[24] N. S. Spinner, K. M. Hinnant, R. Mazurick, A. Brandon, S. L. Rose-Pehrsson and S. G. Tuttle, "Novel 18650 lithium-ion batterysurrogate cell designwith anisotropic thermophysical properties for studying failure events," *Journal of Power Sources 312,* pp. 1-11, 2016.

[25] I. Dinçer, H. S. Hamut and N. Javani, Thermal Management of Electric Vehicle Battery Systems, John Wiley & Sons Ltd, 2017.

[26] "Performance Comparison of Thermal Interface Materials for Power Electronis Applications," in *Applied Power Electronics Conference and Exposition (APEC), 2014 Twenty-Ninth Annual IEEE*, Texas, USA, 2014.

[27] *How does an Electric Car work ? | Tesla Model S.* [Film]. Learn Engineering, 2017.

[28] "Benchmarking the Tesla Model S – A Tour of Ricardo Engineering's Teardown Laboratory," Copper Rotor Induction Motor, 02 11 2014. [Online]. Available: http://www.coppermotor.com/2014/11/benchmarking-the-tesla-model-s-a-tour-of-ricardo-engineerings-teardown-laboratory/?ckattempt=1. [Accessed 30 06 2018].

[29] 3. E. Materials, "3M™ Novec™ 774 Engineered Fluid Product Information," 14 07 2014. [Online]. Available: https://multimedia.3m.com/mws/media/815168O/3mtm-novectm-774-engineered-fluid.pdf. [Accessed 30 06 2018].

[30] Resolved Analytics, "A Comparison of CFD Software Packages," Resolved Analytics, 27 04 2017. [Online]. Available: https://www.resolvedanalytics.com/theflux/comparing-popular-cfd-software-packages. [Accessed 04 06 2018].

[31] 3. E. M. S. Division, "3M™ Novec™ 774 Engineered Fluid," 07 2014. [Online]. Available: https://multimedia.3m.com/mws/media/815168O/3mtm-novectm-774-engineered-fluid.pdf. [Accessed 14 09 2018].

[32] L. Zhang, C. Lyu, G. Hinds and M. Kehua, "Parameter Sensitivity Analysis of Cylindrical LiFePO4 Battery Performance Using Multi-Physics Modeling," *Journal of The Electrochemical Society,* 2014.

[33] H. Schlichting and K. Gersten, Boundary-Layer Theory, Springer, Berlin, Heidelberg, 2017, p. 416–419.

Apendix 1, Comparison of CFD software

To analyze the performance of each cooling method, two CFD software, namely Solidworks Flow Simulation and Star-CCM+, were initially picked to start this research. Although the theoretical model for CFD simulations is the same, different software can give different results and require different computing time and CPU power. This is due to factors such as different meshing and solver algorithm. In this section, the two software Star-CCM and Solidworks Flow Simulation are compared to see which is more accurate and robust.

Flow simulation is an add-on for SolidWorks with the original 3D solid modeling interface. It is primarily used for single phase, steady state, and non-reacting simulations. Star-CCM+ is a multi-disciplinary CFD package with diverse tools mainly used for energy, automotive and aerospace industries [30] . Star-CCM+ is more complex and difficult to use but generally delivers better results. SolidWorks Flow Simulation is primarily designed for ease of use.

Comparison of Solidworks Flow Simulation and Star-CCM+ simulation results:

For this matter, a simple model with five batteries with a cooling tube in the middle was made. The material properties, the coolant flow, and other inputs were set the same in both software.

The geometry was made in SolidWorks as it was a more convenient CAD software and later it was imported to Star-CCM+.

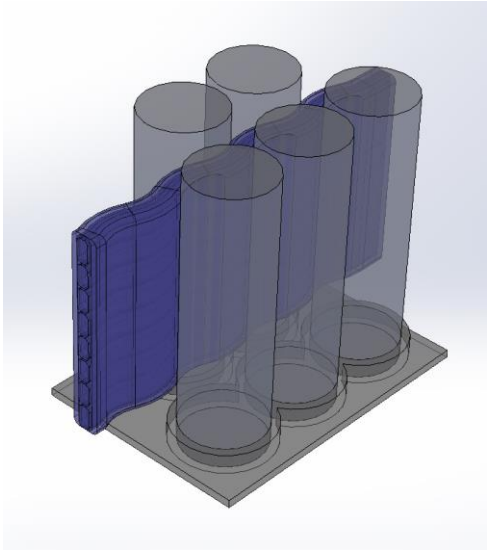

Figure 49. Model geometry

The first step for simulation is to create a mesh to run the solver on. In this case, Star-CCM+ offers a unique meshing system where it enables the user to customize the cells based on the importance and criticality of different parts of the geometry. For this simulations, Surface Remesher was used so that there would be as little loss of surface details as possible. Surface meshing prepares the geometry for volume geometry. The aluminum tube, thermal interface material, and the clamshell edges are modeled using a Thin Mesher that enables more detailed uniform cells that capture heat gradient in these parts. The inner volume of the geometry is modeled using polyhedral meshes which are recommended for heat transfer problems.

In SolidWorks, the meshing process is much simpler. The geometry is cut into cubes, therefore, the size of the cells have to be very small to properly cover the all the thin layers and edges.

The images below show the cell composition of the same geometry in each program.

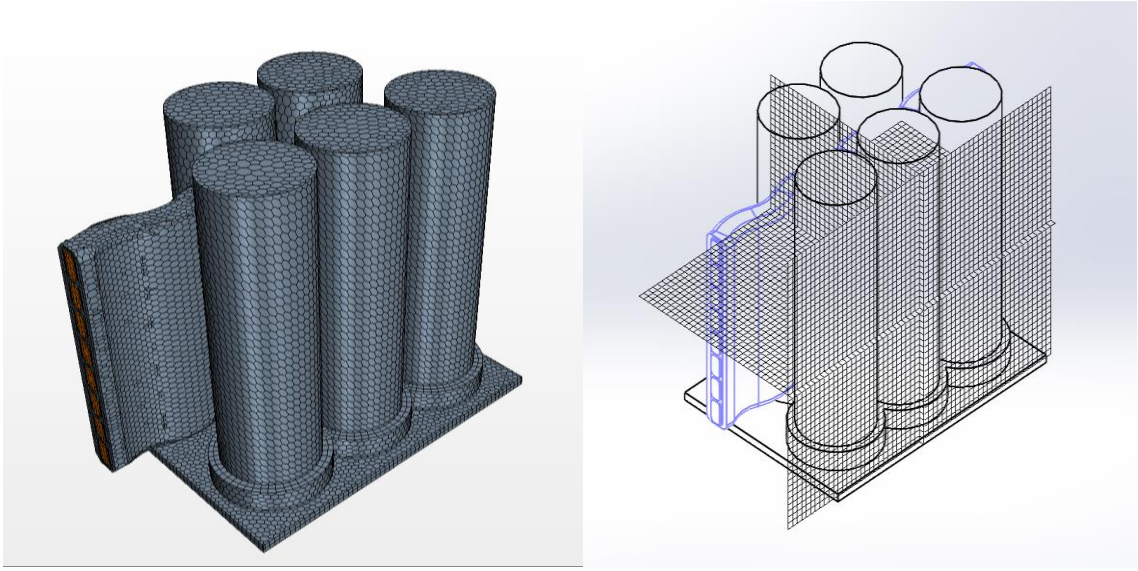

Figure 50. Star-CCM+ meshing (left), Solidworks Flow Simulation meshing (right)

As can be seen in the image above the concentration of the cells are higher at the intersection between the Cooling tube and the cells which is more important due to the higher thermal gradient at that point. This enables more efficient and faster simulation results.

Using the more efficient meshing algorithm of Star-CCM+ it was possible to mesh the same geometry with five times fewer cells compared to SolidWorks while maintaining the important cells.

The physical and initial conditions are as shown in the table below:

Initial Temperature	20 °C
Coolant Inlet Temperature	20 °C
Coolant Inlet Velocity	0.1 m/s
Heat Generation	0.2 w/Cell
Cell conductivity	Kr = 1 w/m*k Ka = 25 w/m*k

The models were fully solved and the with the following properties.

Software	Solidworks Flow simulation	Star-CCM+
Number of Cells	525495	103244
Meshing model	Cubes	-Surface Remesher -Polyhedral Mesher -Thin Mesher
Iterations	144	1400
CPU Time per Iteration	16 s	2,5 s
CPU Time	40 min	1 h

The time per each iteration is clearly much smaller for Star-CCM due to the lower number of meshes. On the other hand, more, iterations were required to have a more stable result. This is something that needs to be fixed by the user manually to have faster convergence and lower residuals faster.

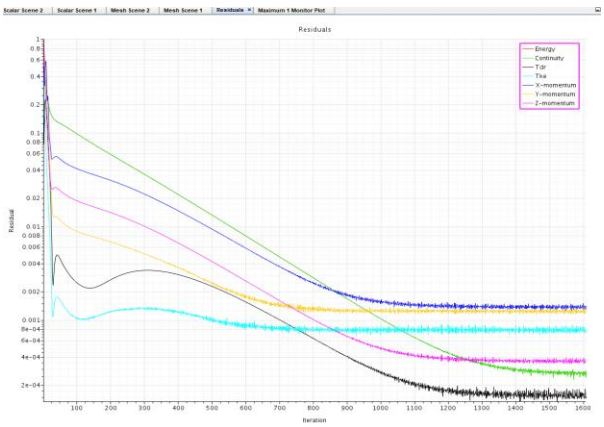

Figure 51. Residuals in Star-CCM+

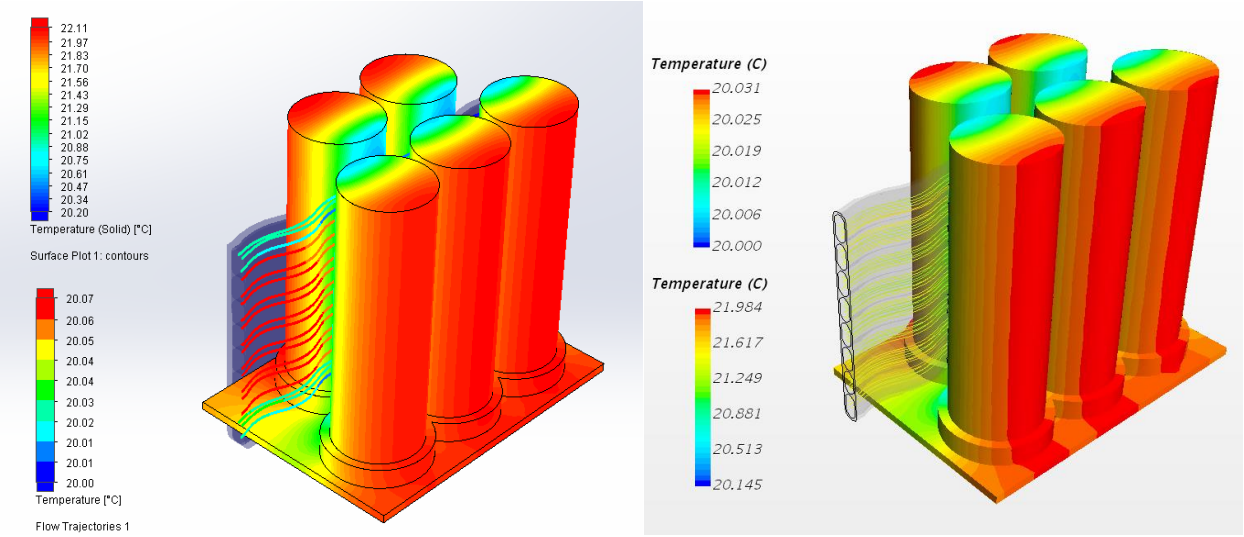

Figure 52. Thermal distrebution in Star-CCM+(right) and Solidworks (left)

The results are close to each other. The highest temperature reached in the batteries is in 21,9 ^{o}C in Star-CCM+ and 22,1^{o}C in Solidworks. The maximum coolant temperature is almost double in Solidworks.

Overall it was seen that Star CCM is more complex and difficult to use, but generally delivers better results. SolidWorks Flow Simulation is primarily designed for ease of use.

Appendix 2. Mesh Study

To find the right mesh size, the model for simulation cooling was repeated several times with different mesh base size. The results were compared in two parameters:

- Coolant temperature difference
- Maximum cell temperature

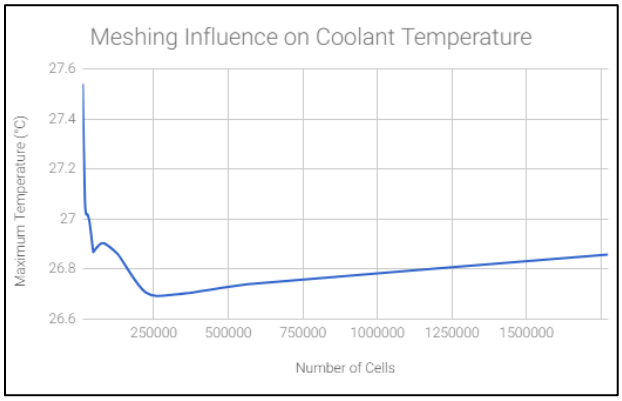

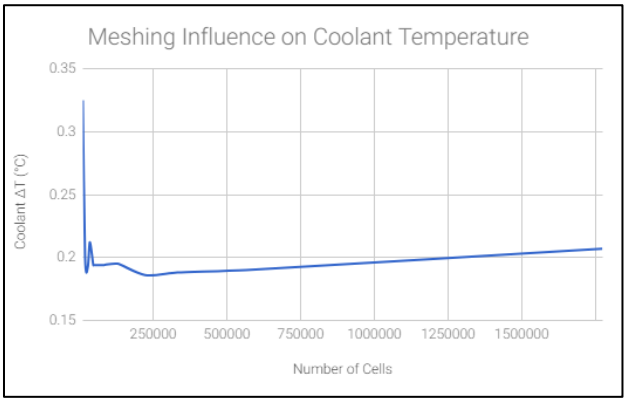

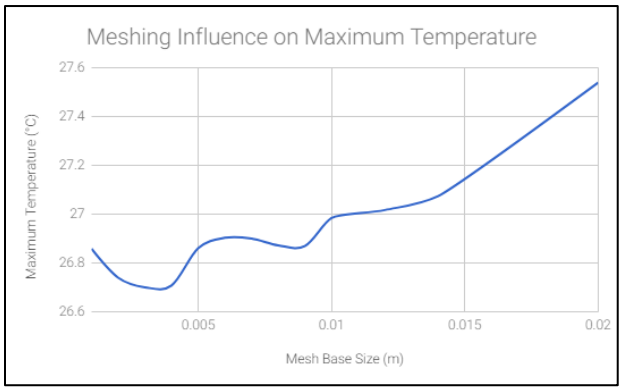

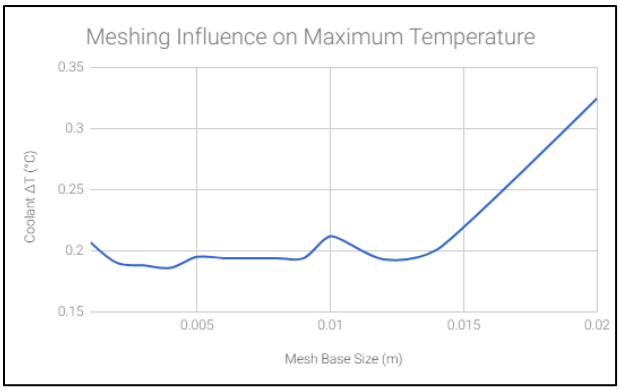

The base size of 0,005m was chosen as a moderate value that gives the right result while keeping the number of meshes low.